

AD-A251 871



(2)

CONTRACT NO.: DAMD17-89-Z-9025

TITLE: New Therapeutic Modalities of Retinal Laser Injury

PRINCIPAL INVESTIGATOR: Mark O.M. Tso

PI ADDRESS: University of Illinois at Chicago, Dept. of Ophthalmology
1855 W. Taylor, L217
Chicago, IL 60612

REPORT DATE: March 31, 1992

TYPE OF REPORT: FINAL

PREPARED FOR: U.S. ARMY MEDICAL RESEARCH AND DEVELOPMENT COMMAND
FORT DETRICK
FREDERICK, MARYLAND 21702-5012

DISTRIBUTION STATEMENT: Approved for public release;
distribution unlimited

DTIC
ELECTE
31 3 1992
S A D

92-16367



92 6 22 004

REPORT DOCUMENTATION PAGE

Form Approved
OMB No. 0704-0

1a. REPORT SECURITY CLASSIFICATION unclassified			1b. RESTRICTIVE MARKINGS	
2a. SECURITY CLASSIFICATION AUTHORITY			3. DISTRIBUTION/AVAILABILITY OF REPORT approved for public release; distribution unlimited	
2b. DECLASSIFICATION/DOWNGRADING SCHEDULE			5. MONITORING ORGANIZATION REPORT NUMBER(S)	
4. PERFORMING ORGANIZATION REPORT NUMBER(S)			7a. NAME OF MONITORING ORGANIZATION	
6a. NAME OF PERFORMING ORGANIZATION University of Illinois at Chicago		6b. OFFICE SYMBOL (If applicable)	7b. ADDRESS (City, State, and ZIP Code)	
6c. ADDRESS (City, State, and ZIP Code) Board of Trustee 833 S. Wood Street Chicago, IL 60612			9. PROCUREMENT INSTRUMENT IDENTIFICATION NUMBER DAMD17-89-Z-9025	
8a. NAME OF FUNDING/SPONSORING ORGANIZATION U.S. Army Medical Research & Development Command		8b. OFFICE SYMBOL (If applicable)	10. SOURCE OF FUNDING NUMBERS	
8c. ADDRESS (City, State, and ZIP Code) Fort Detrick Frederick, MD 21702-5012		PROGRAM ELEMENT NO. 61102A	PROJECT NO. 3MI-61102BS15	TASK NO. CF
			WORK UNIT ACCESSION DA318244	
11. TITLE (Include Security Classification) New Therapeutic Modalities for Retinal Laser Injury				
12. PERSONAL AUTHOR(S) Tim T. Lam, Ph.D., and Mark O.M. Tso, M.D.				
13a. TYPE OF REPORT FINAL		13b. TIME COVERED FROM 3-1-89 TO 3-1-92		14. DATE OF REPORT (Year, Month, Day) 1992 March 31
15. PAGE COUNT 72				
16. SUPPLEMENTARY NOTATION				
17. COSATI CODES			18. SUBJECT TERMS (Continue on reverse if necessary and identify by block number)	
FIELD	GROUP	SUB-GROUP	Laser, Retina, Injury, Treatment, Corticosteroids, Methylprednisolone, tissue plasminogen activator, sub-retinal hemorrhage, RA 3	
09	03			
06	04			
19. ABSTRACT (Continue on reverse if necessary and identify by block number)				
<p>Efficacies of three different regimens of high dose of methylprednisolone (MP) treatment on laser-induced non-hemorrhage retinal injury and tissue plasminogen activator (t-PA) in sub-retinal hemorrhage laser injury were evaluated in a sub-human primate model and a rat model respectively. Clinical, histopathological, and morphometric criteria were employed for evaluating the efficacy of MP. High dose and prolonged treatment (4 days) was the most effective regimen while high dose for 8 hours showed limited effect in non-hemorrhagic retinal injury. Intravitreal t-PA showed no apparent beneficial effect in sub-retinal hemorrhage after laser injury. Hence, patients with laser retinal injury may benefit from high dose MP treatment for an appropriate period of time.</p>				
20. DISTRIBUTION/AVAILABILITY OF ABSTRACT <input type="checkbox"/> UNCLASSIFIED/UNLIMITED <input checked="" type="checkbox"/> SAME AS RPT <input type="checkbox"/> DTIC USERS			21. ABSTRACT SECURITY CLASSIFICATION unclassified	
22a. NAME OF RESPONSIBLE INDIVIDUAL Mary Frances Bostian			22b. TELEPHONE (Include Area Code) 301-619-7325	22c. OFFICE SYMBOL SGRD-RMI-S

FOREWORD

Opinions, interpretations, conclusions and recommendations are those of the author and are not necessarily endorsed by the U.S. Army.

N/A Where copyrighted material is quoted, permission has been obtained to use such material.

N/A Where material from documents designated for limited distribution is quoted, permission has been obtained to use the material.

N/A Citations of commercial organizations and trade names in this report do not constitute an official Department of the Army endorsement or approval of the products or services of these organizations.

yes ^{WJ} In conducting research using animals, the investigator(s) adhered to the "Guide for the Care and Use of Laboratory Animals," prepared by the Committee on Care and Use of Laboratory Animals of the Institute of Laboratory Animal Resources, National Research Council (NIH Publication No. 86-23, Revised 1985).

N/A For the protection of human subjects, the investigator(s) have adhered to policies of applicable Federal Law 45CFR46.

N/A In conducting research utilizing recombinant DNA technology, the investigator(s) adhered to current guidelines promulgated by the National Institutes of Health.

Accession For	
NTIS CRA&I	<input checked="" type="checkbox"/>
DTIC TAB	<input type="checkbox"/>
Unannounced	<input type="checkbox"/>
Justification	
By	
Distribution /	
Availability Codes	
Dist	Avail and/or Special
A-1	

W. J. [Signature] 4/10/92
PI Signature Date



TABLE OF CONTENTS

Front Cover	i.
DD Form 1473	ii.
Foreword	iii.
Table of Contents	iv.
List of Illustrations	v.
Summary	1
Chapter 1: Introduction	4
1.1: Incidence of retinal laser injury	4
1.2: Experimental treatment of retinal laser injury	4
1.3: Clinical therapy	4
1.4: Our hypothesis and approaches	4
Chapter 2: Accidental laser injury to the human retina	7
2.1: Introduction	7
2.2: Case 1	7
2.3: Case 2	8
2.4: General comments	9
2.5: Clinical course	10
2.6: Implications	10
Chapter 3: Sub-human primate model of non-hemorrhagic retinal laser injury and evaluation of the efficacy of high doses of methylprednisolone	17
3.1: Studies of retinal laser lesions	17
3.2: Choice of methylprednisolone	17
3.3: Methods	18
3.4: Results	20
3.5: Comment	24
Chapter 4: Ultrastructural modification by high dose methylprednisolone on laser-induced injury of the monkey retina	41
4.1: Introduction	41
4.2: Method	41
4.3: Results	41
4.4: Comments	45
Chapter 5: Evaluation of efficacy of t-PA in subretinal hemorrhage induced by retinal laser injury in rats	59
5.1: Pathophysiology of vitreal or retinal hemorrhage	59
5.2: Treatment of intravitreal and subretinal hemorrhage	59
5.3: Earlier experimental treatments	59
5.4: Tissue plasminogen activator (t-PA)	60
5.5: Method	61
5.6: Results	61
5.7: Comments	62
Concluding Remarks	65
References	66
Acknowledgments	71

LIST OF ILLUSTRATIONS

Diagram 1:	Working hypothesis	6
Figure 2.1:	Transmittance spectrum of the protective goggles for Argon laser	11
Figure 2.2:	Amsler charts of patient #1	12
Figure 2.3:	Fundus picture & fluorescein angiogram of the right eye of patient #1	13
Figure 2.4:	Amsler charts of patient #2	14
Figure 2.5:	Fundus picture & fluorescein angiogram of the left eye of patient #2	15
Figure 2.6:	Fundus picture & fluorescein angiogram of the right eye of patient #2	16
Diagram 2:	Proposed sites of action of methylprednisolone and t-PA	29
Diagram 3:	Schedule of administering methylprednisolone	30
Diagram 4:	Illustration of morphometric indice for laser lesion	31
Figure 3.1:	Histopathologic changes of Grade II laser lesions	32
Figure 3.2:	Histopathologic changes of Grade III laser lesions	33
Figure 3.3:	Morphometric changes of the control Grade II lesions	34
Figure 3.4:	Morphometric changes of the control Grade III lesions	35
Figure 3.5:	Morphometric indice linear dependency on the energy setting of Argon laser	36
Figure 3.6:	Ophthalmoscopic & FANG appearance of Grade III lesions at 3 days	37
Figure 3.7:	Ophthalmoscopic & FANG appearance of Grade III lesions at 10 days	38
Figure 3.8:	Histopathologic studies of retinal lesions	39
Figure 3.9:	Effects of different treatment regimens on laser-induced lesions	40
Figure 4.1:	Center of the control lesion at 3 days after laser photocoagulation	49
Figure 4.2:	Center of the MP-treated lesion at 3 days after laser photocoagulation	50
Figure 4.3:	Periphery of the control lesion at 3 days after laser photocoagulation	51
Figure 4.4:	Outer plexiform layer in the control lesion 3 days after laser photocoagulation	52
Figure 4.5:	Periphery of the MP-treated lesion at 3 days after laser photocoagulation	53
Figure 4.6:	Paralesional area OPL in the control lesion 3 days after photocoagulation	54
Figure 4.7:	Center of the control lesion at 10 days after laser photocoagulation	55
Figure 4.8:	Center of the MP-treated lesion at 10 days after laser photocoagulation	56
Figure 4.9:	OPL in the control lesion at 10 days after laser photocoagulation	57
Figure 4.10:	OPL layer in the MP-treated lesion at 10 days after laser photocoagulation	58
Figure 5.1:	Histologic section of control and t-PA-treated subretinal hemorrhage lesions	63
Figure 5.2:	Morphometry of laser lesions with subretinal hemorrhage with and without t-PA treatment	64

University of Illinois At Chicago Eye Center

Georgiana Dvorak Theobald Ophthalmic Pathology Laboratory

Director: Mark O.M. Tso, M.D.

New Therapeutic Modalities of Retinal Laser Injury (DAMD17-89-Z-9025)

**(DARPA program on eye and sensor protection against the
battlefield laser threat)**

Final report

SUMMARY

New Therapeutic Modalities for Retinal Laser Injury

With the widespread use of laser equipment in civilian and military settings, the incidence of retinal injury by laser has been growing. Presently, there are no established guidelines of treatment for these injuries and there are only limited controlled quantitative studies of effective therapeutic modalities. The primary goals of this contract are to evaluate the efficacy of glucocorticoid and tissue plasminogen activator (t-PA) in the treatment of laser induced retinal injury.

The following steps were undertaken to achieve our goals:

- (1) to develop animal models of retinal laser injury with or without subretinal hemorrhage; and
- (2) to assess the respective efficacy of glucocorticoid and t-PA in these retinal lesions.

In addition, during this contract period, we were able to document the clinical course of two patients with retinal laser injury.

This report consisted of 5 chapters with concluding remarks and references at the end. Relevant background, our hypothesis, and approaches were summarized in Chapter 1. We proposed that secondary cell damage occurs in the retina surrounding a central necrotic zone of laser injury and that appropriate medical treatment will ameliorate the secondary damage and limit the retinal lesion. This hypothesis evolved from our understanding of neuronal cell injury/death in different CNS models such as cerebral ischemia and spinal cord injury, in which various agents such as calcium antagonists and N-methyl-D-aspartate receptor antagonists will rescue injured neuronal cells.

In Chapter 2, we described two patients at the macula clinic of the UIC Eye Center who suffered accidental injury to the retina by Nd:YAG laser. These case studies gave us new information on the clinical course of retinal injury after laser. Both cases shared remarkable similarities in their clinical course showing retinal burns with initial subretinal/retinal or vitreal hemorrhage, retinal edema with decrease in vision, gradual reabsorption of blood, decrease of edema, and remarkable improvement of vision, but with residual macular hole formation.

To test our hypothesis, we developed retinal models of laser injury for quantitative evaluation of efficacy of agents for the rescue of injured retinal cells. In the first part of Chapter 3, we described a sub-human primate (*Cynomolgus* monkey) model of retinal laser injury by a continuous wave Argon laser (CW Argon). Clinical, histopathologic, and morphometric methods

to document the laser injury were employed. Morphometric indices were established for the quantitative evaluation of retinal repair. We observed remarkable healing of the retina after injury. This observation explains the improvement of vision in patients with retinal laser injury over a period of months.

Methylprednisolone (MP) was selected among a list of neuronal cell rescuers because of its proven efficacy in humans. Dramatic beneficial effects of methylprednisolone in patients with acute spinal cord injury, when given a loading dose of 30 mg/kg followed by a maintenance dose of 5.4 mg/kg/hr, were reported in the Second National Clinical Trial Study of Acute Spinal Cord Injury (1990). Our evaluation of similar administration of MP for retinal laser injury in monkeys was described in the second part of Chapter 3. We tested three treatment regimens with methylprednisolone: (1) prophylactic and continued treatment for 3 days after injury; (2) immediate treatment for 4 days following injury; and (3) immediate treatment for 8 hours following injury. All regimens were found to be effective with clinical and histopathologic criteria. However, with morphometric indices, only prophylactic and continued treatment for 3 days after injury (regimen 1) and immediate treatment for 4 days following injury (regimen 2) showed significant beneficial effects while immediate treatment for 8 hours showed no significant beneficial effect. Hence, early high dose and continuous treatment with methylprednisolone for 4 days is effective while short time (8 hours) treatment showed limited efficacy.

Ultrastructural studies to examine the cellular responses after injury provided further insight in the pathogenetic mechanisms of cell death. Electron microscopic study of the retinal lesions with and without methylprednisolone treatment was described in Chapter 4. Treatment with methylprednisolone limited the occlusion of chorioidal vessels, the proliferation of retinal pigmented epithelium, and the infiltration of macrophages after retinal laser injury. Hence, specific therapeutic approaches may be targeted to these pathologic changes for maximum rescuing effects.

Chapter 5 described our evaluation of the efficacy of tissue plasminogen activator (t-PA) in subretinal hemorrhage in rat laser lesions. A model of subretinal hemorrhage was induced in the rat by a continuous wave Argon laser (CW Argon) because of the need for larger sample sizes due to the expected variations in hemorrhagic injury. Recombinant t-PA was selected because of its purity, specificity, and minimum toxicity. Our study showed that there was no apparent beneficial effect of t-PA on laser-induced subretinal hemorrhage when evaluated at 4 days after injury.

In summary, we documented two cases of retinal laser injury in human patients. A subhuman primate model for quantitative evaluation of efficacy of various agents for non-hemorrhagic injury to the retina by laser was established. We showed that a high dose (30 mg/kg plus 5.4 mg/kg/hr) of methylprednisolone was beneficial for non-hemorrhagic injury to the monkey retina. We also established a rat model for quantitative evaluation of efficacy of various

agents for subretinal hemorrhage by laser. Recombinant t-PA given at 25 ug intravitreally was not effective in this model.

Chapter 1

INTRODUCTION

1.1 Incidence of retinal laser injury

Since the first report of accidental laser burns of the macula by Rathkey¹, there have been other scattered reports of laser injury to the retina. Wolfe² summarized all the laser retinal injuries reported in the literature up to 1985 and reported a total of 23 cases. Of the 23 cases, 7 involved YAG laser operating at 1064 nm wavelength. All cases that involved the YAG laser caused retinal/subretinal or vitreous hemorrhage. Of the 7 cases reported, 3 cases were reported to develop macular holes and 1 case resulted in macular pucker formation. Since then, there has been an increase in reported incidences including one case each by Kearney et al³, by Friedmann⁴ and by Anderberg⁵, 6 cases by Gabel⁶, as well as 19 cases referred by Cai et al⁷, 2 cases by Cai et al⁷, 29 cases from 1976 to 1986 by Liu et al⁸, and 3 cases by Whitacre et al⁹. In addition, laser injuries to the retina by weapons have been reported in the recent Persian Gulf War. It seems apparent that with the widespread use of laser in military, medical, and experimental settings, the incidence of laser injury to the retina will continue to grow. However, currently there are no established guidelines for treatment.

1.2 Experimental treatment of retinal laser injury

There have been few studies on the treatment of laser-induced retinal injury. Ishibashi et al¹⁰ reported the inhibition of subretinal neovascularization by dexamethasone in laser-induced retinal lesions in monkeys. Belkin et al¹¹ studied the use of urokinase treatment in laser-induced vitreous hemorrhage in rabbits and concluded that urokinase did not accelerate the absorption of blood from the vitreous, but prevented the development of severe vitreous fibrosis, which followed the hemorrhage in some of the control eyes.

1.3 Clinical therapy

Clinically, of the 23 patients reported by Wolfe², 10 had steroid therapy. In some reported cases, improvement was reported after steroid therapy. However, there has been no controlled study to demonstrate the efficacy of steroid therapy.

1.4 Our hypothesis and approaches

The lack of progress in developing new and rational approaches to therapy of laser induced retinal injury may be partially due to the belief that the retinal injury is usually too severe to be treated. Furthermore, pathophysiology of laser injury to the retina is not well studied. However, with the recent improved understanding of the pathophysiology of neuronal cell injury in various animal models and of the roles of intracellular calcium, excitotoxicity and lipid peroxidation in neuronal cell death, new therapeutic approaches to neuronal cell injury are proposed^{12,13}. Studies have shown that various agents that inhibit the elevation of intracellular calcium levels¹², inhibit receptors of the endogenous excitatory amino acids¹² and diminish lipid peroxidation¹³

may prevent secondary cell death after the initial insult to the central nervous system. The retina, being part of the central nervous system, may show similar behavior as in the brain or spinal cord after injury. Our initial hypothesis is that there are secondary injuries around the initial laser insult and that these secondary processes may be modulated by appropriate agents. Therefore, our approach is to limit these secondary changes in the retina (Diagram 1).

To achieve the primary objective of this research contract, which was to develop new therapeutic modalities for retinal laser injury, we sought to

- (1) document the clinical course of laser induced retinal injury (Chapter 2);
- (2) establish an animal model for examining the efficacy of various test agents for non-hemorrhagic retinal lesions (Chapter 3);
- (3) quantitatively evaluate the efficacy of methylprednisolone on these non-hemorrhagic retinal laser lesions (Chapter 3);
- (4) improve our understanding of the tissue responses after laser injury with and without methylprednisolone treatment by ultra-structural studies (Chapter 4).
- (5) establish an animal model for examining the efficacy of various therapeutic agents for hemorrhagic retinal laser injury (Chapter 5); and
- (6) evaluation of the efficacy of tissue plasminogen activator (t-PA) on sub-retinal hemorrhagic laser lesions of the retina (Chapter 5).

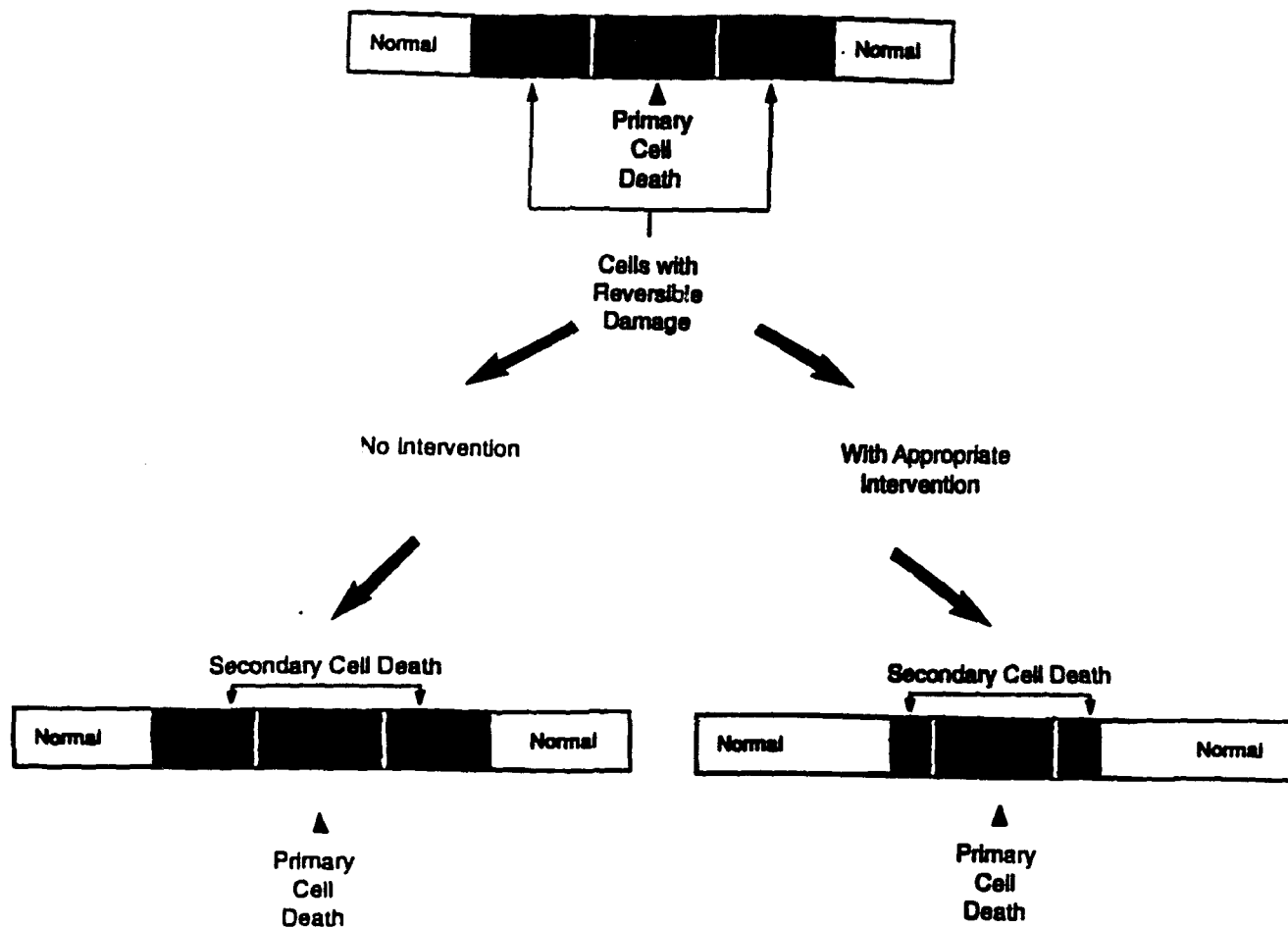


Diagram 1: Working hypothesis

Chapter 2

Accidental laser injury to the human retina

2.1 Introduction

Even though clinical manifestations of laser induced retinal injury in human has been described in the literature, and as the conditions of injury and the tissue responses greatly vary, it is important to document all available cases in a systematic manner so that a comprehensive view of the injury, and hence better strategy for therapy, may be developed. In this contract period, we followed two patients from the Macula clinic of the UIC Eye Center with accidental laser injury to the retina.

2.2 CASE 1

A 23 year-old-male physics graduate student of Asian descent was experimenting with frequency-mixing of laser beams. The laser involved in the accident was a pulsed Nd:YAG laser with a full power of 2 W and a spot size of 1 mm². It was operating at 1064 nm, 10 Hz and 10 nsec pulses. While the patient was adjusting the position of the KDP crystal for mixing, the beam from the Nd:YAG laser was reflected from the crystal surface to the patient's right eye accidentally. The reflected beam was estimated to be approximately 5% of the incident light. According to the patient's calculation, the energy reaching the cornea surface was approximately 5 mj/pulse. Immediately after the exposure, the patient reported dark brown objects floating at the center of the vision in his right eye. The floating objects scattered gradually and a scotoma remained at the center of his vision. No pain was reported, but the patient experienced a shockwave. The patient reported wearing protective goggles for argon laser which might have a similar transmittance spectrum of that reported in case 2 (see Fig. 2.1). Within 10 minutes the patient was examined by a physician.

His visual acuities were recorded to be 20/200 (OD) and 20/15 (OS). The patient was reported to have distorted central vision in the right eye. Laser-induced hemorrhage was observed. He was examined 2 weeks later by an ophthalmologist. His vision had improved to 20/40 in the right eye and was 20/20 in the left eye. Intraocular pressure was 22 and 17 mm Hg in the right and left eye respectively. Ophthalmologically, a yellow central necrotic area at the fovea with radiating folds of the retina was noted in the right eye. No hemorrhage was reported, suggesting that the hemorrhage seen earlier after the accident might have been resolved within the two week interval. Fundus examination of the left eye was normal. The patient was seen at our Macular Clinic 6 weeks after the accident. His visual acuity had improved to 20/25 in the right eye and remained 20/20 in the left eye. Amsler Grid examination showed paracentral scotoma and patient reported metamorphopsia adjacent to the central fixation point (Fig. 2.2A). A mild

subepithelial opacity was noted at the temporal inferior quadrant of the right cornea. The lenses were clear with no focal opacity. Intraocular pressures were 16 mm Hg (OD) and 15 mm Hg (OS). Fundus examination of the right eye showed a large pigmented scar in the macula, with a hole centrally and surrounding shallow serous retinal detachment (Fig. 2.3A). Preretinal fibrosis with retinal folds was also observed in the macular area. A small choroidal vessel was noted at the bottom of the macula hole (Fig. 2.3A). Fluorescein angiography (FANG) (Fig. 2.3B) showed no fluorescein leakage and focal staining at the macular hole. He was given 15 mg beta-carotene t.i.d. The patient returned for follow-up after 1 month. His visual acuity was 20/30 in the right eye and 20/20 in the left eye. In his right eye, paracentral scotoma and metamorphopsia were unchanged. Fundus examination of the right eye showed chorioretinal scar with more prominent pigmentation compared to previous visit. Depigmentation in the fovea persisted (Fig. 2.3C). Preretinal membrane over the macula and a full-thickness macula hole were noted as before. FANG confirmed the retinal pigmented epithelial (RPE) staining of a macula hole and pigmented scar (Fig. 2.3D). No fluorescein leakage was noted. The patient returned for further examination 3 and 1/2 months after the accident. His visual acuity remained at 20/30 in the right eye and 20/20 in the left eye. He continued to complain of an inferior nasal scotoma and metamorphopsia (Fig. 2.2B). However, the scotoma appeared to have decreased in size. Fundus examination showed a centrally depigmented area in the fovea and a spot of pigmented area at the center larger than previously seen (Fig. 2.3E). The premacular fibrosis appeared to improve. The macula was flattened showing minimum traction as compared to the last visit. Fluorescein angiography showed a hyperfluorescent ring corresponding to the edge of the macula hole.

2.3 CASE 2

The patient was a 29 year-old female electrical engineering graduate student of Asian descent. The accident happened during a spectroscopic experiment using a pulsed Nd:YAG laser with an output power of 50 mJ/pulse operating at 1064 nm, 10 nano sec/pulse and a spot size of 5 mm diameter. The patient reported wearing goggles which were later examined in our laboratory to have more than 90% transmittance at wavelengths above 530 nm (Fig. 2.1). The patient complained of immediate metamorphopsia with blurred vision in her left eye. She was seen 2 days later by an ophthalmologist who reported central scotoma extending nasally in the affected left eye. Her visual acuity was 20/20 in the right eye and 20/60 in the left eye. Fundus examination of the left eye showed an eccentric macular burn with surrounding edema and hemorrhage. The patient attended our Macular Clinic 1 week after the accident. Her vision was 20/20 in the right eye and 20/50 in the left eye (OS). The latter eye had central metamorphopsia, but no scotoma (Fig. 2.4A). Intraocular pressure (IOP) was 14 mm Hg in both eyes. Fundus examination of the left eye showed a laser burn at 2^O temporal to the fovea (Fig. 2.5A). There was a dark red

discoloration in the fovea, interpreted to be subretinal and subretinal pigment epithelium (sub-RPE) hemorrhage. Small chorioretinal scars were also noted in the paramacular area of the right eye (Fig 2.6). Fluorescein angiography showed no active fluorescein leakage in both eyes; but there was a hypofluorescence area at the macula consistent with subretinal and sub-RPE hemorrhage (Fig. 2.5B). The patient was given antioxidants of ascorbic acid and Beta-carotene, and was re-examined 1 month after the accident and her visual acuity remained 20/50 in the left eye. The area of central metamorphopsia decreased with a scotoma in the inferior-nasal visual field (Fig. 2.4B). Fundus examination showed that the subretinal hemorrhage had spread (Fig. 2.5C). Early organization of the hemorrhage with yellowish fibrosis was noted. Fluorescein angiogram was unchanged (Fig. 2.5D). The patient returned 2 and 1/2 months after the accident and her visual acuity improved to 20/30 in the left eye. Amsler chart showed further decrease of the metamorphopsia with a persistent gray scotomatous area (Fig. 2.4C). Fundus examination showed reabsorption of subretinal hemorrhage (Fig. 2.5E). A reddish lesion remained at the parafovea area in the temporal superior quadrant. A lamella hole was developing at the inferior nasal parafoveal area. FANG showed RPE staining of the lesion in the temporal superior quadrant (Fig. 2.5F).

2.4 General comments

Two cases of accidental injury by reflected laser beams were reported. The reflection in the first case was by a KDP crystal, and the other by an unspecified surface. Both patients claimed to wear laser-safety goggles, but with the wrong cut-off wavelength. Instead of wearing the KG3-5 goggles which are readily available for the 1064 nm wavelength, the patients were wearing protective goggles for argon lasers. The argon safety goggles transmit more than 90% in the infrared region (Fig. 2.1). Both patients were graduate students in the physical science departments, supposedly knowledgeable of the possible dangers of laser injury to the retina. However, it is apparent that appropriate safety measurements were not followed. It was not clear why the subjects wore the wrong goggles. Suffice to say that these two cases clearly demonstrate the insufficiency of laser safety education, the lack of standardized procedures, and improper supervision for personnel involved in laser handling.

Careful examination of the second patient's right eye showed a chorioretinal scar at the inferior temporal quadrant of the paramacular area (Fig. 2.6). Although the patient did not complain of laser injury to the right eye previously, it appeared that the scar might be from previously unreported laser injuries. Gabel et al⁶ also reported observations of unnoticed laser burn in workers involved in laser-handling under routine eye examination. Hence, it seems that the incidence of accidental laser injury to the retina may be much higher than expected.

2.5 Clinical course

In both cases, the clinical course showed remarkable similarities. Initially, subretinal, sub-RPE, or vitreal hemorrhage was reported with central scotoma and metamorphopsia. The initially dramatic decrease in visual acuity gradually improved over a couple of months. The subretinal and/or sub-RPE hemorrhage was gradually absorbed over a period of time, although in the first case it was absorbed more rapidly (in a matter of 2 weeks and the rapid resolution of the hemorrhage may be associated with the full thickness retinal necrosis and escape of subretinal blood to the vitreous cavity). Chorioretinal scars were observed with gliosis/fibrosis. In both cases, macular holes were formed. Visual acuity in both patients improved dramatically over the ensuing months of follow-up. These clinical courses are comparable to the reports of experimental and clinical laser injury to the retina. Manning et al¹⁴ reported that macular puckers, macular holes and cysts are sequelae of YAG laser injury. It is interesting to know that in both our cases, the macular holes were formed away from the apparent laser burn site.

2.6 Implications

From these clinical studies, it seems rational to design therapy to retinal laser injury in the following ways: (1) to promote rapid resorption of sub-retinal/retinal/vitreous hemorrhage; (2) to promote healing and repair of the retina; (3) to limit chorioretinal scar formation; and (4) to prevent retinal hole formation.

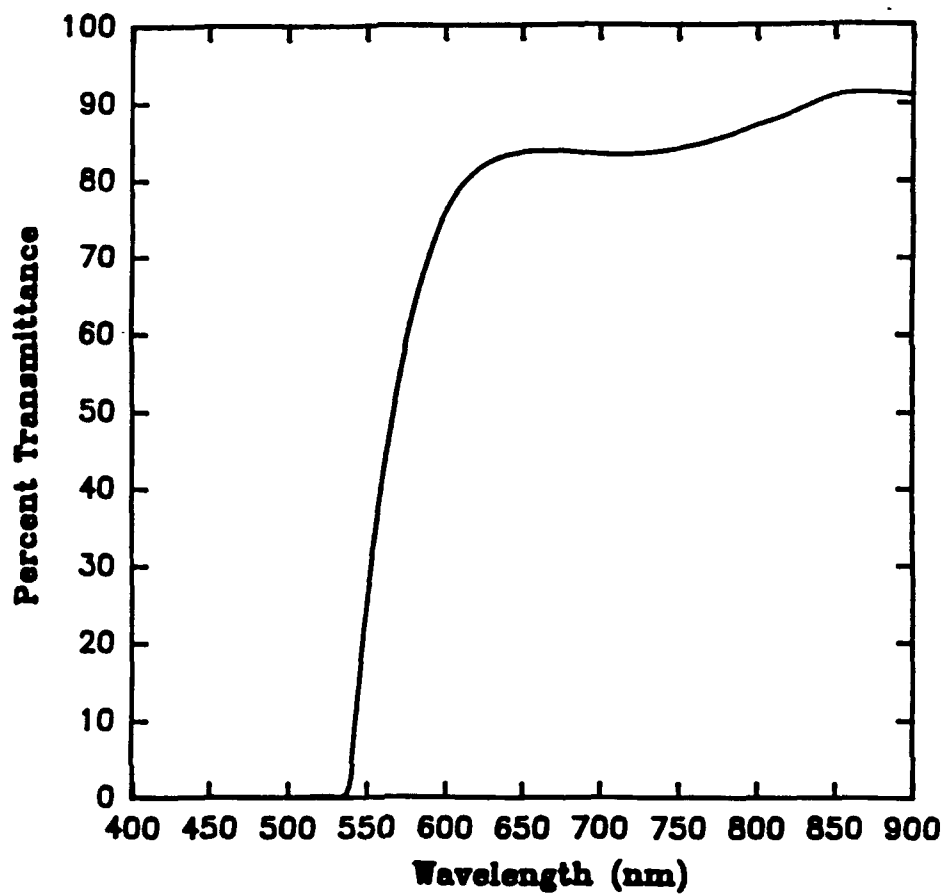


Fig 2.1 Transmittance spectrum of the protective goggles for Argon laser

AMSLER RECORDING CHART

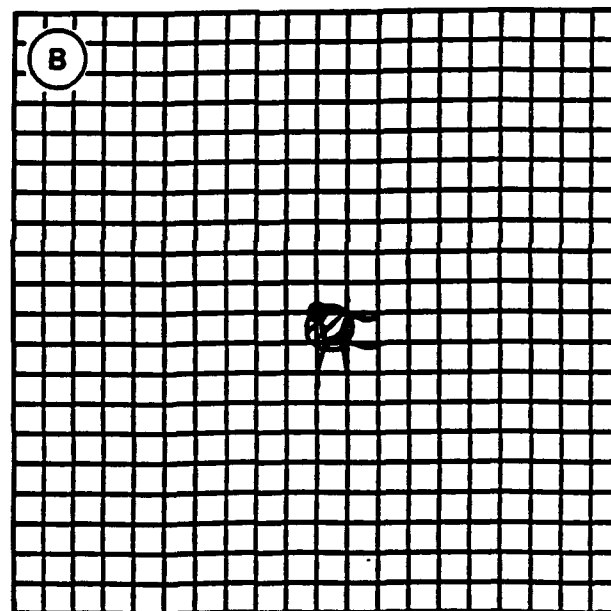
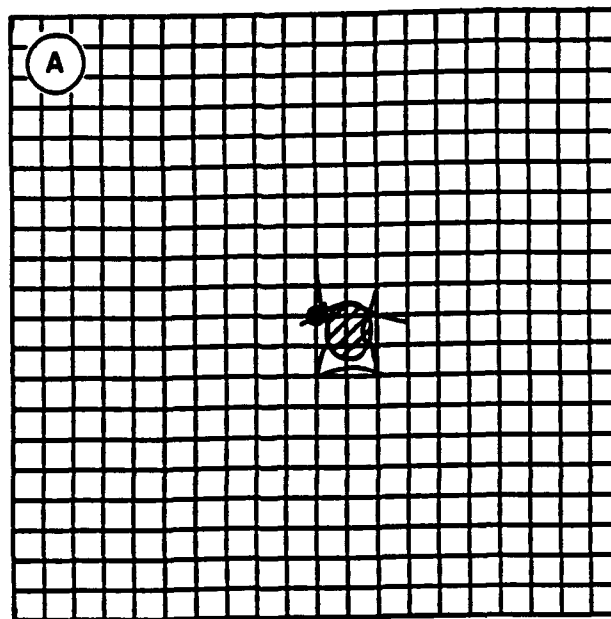


Fig 2.2: Amsler charts of patient #1. See text for description.

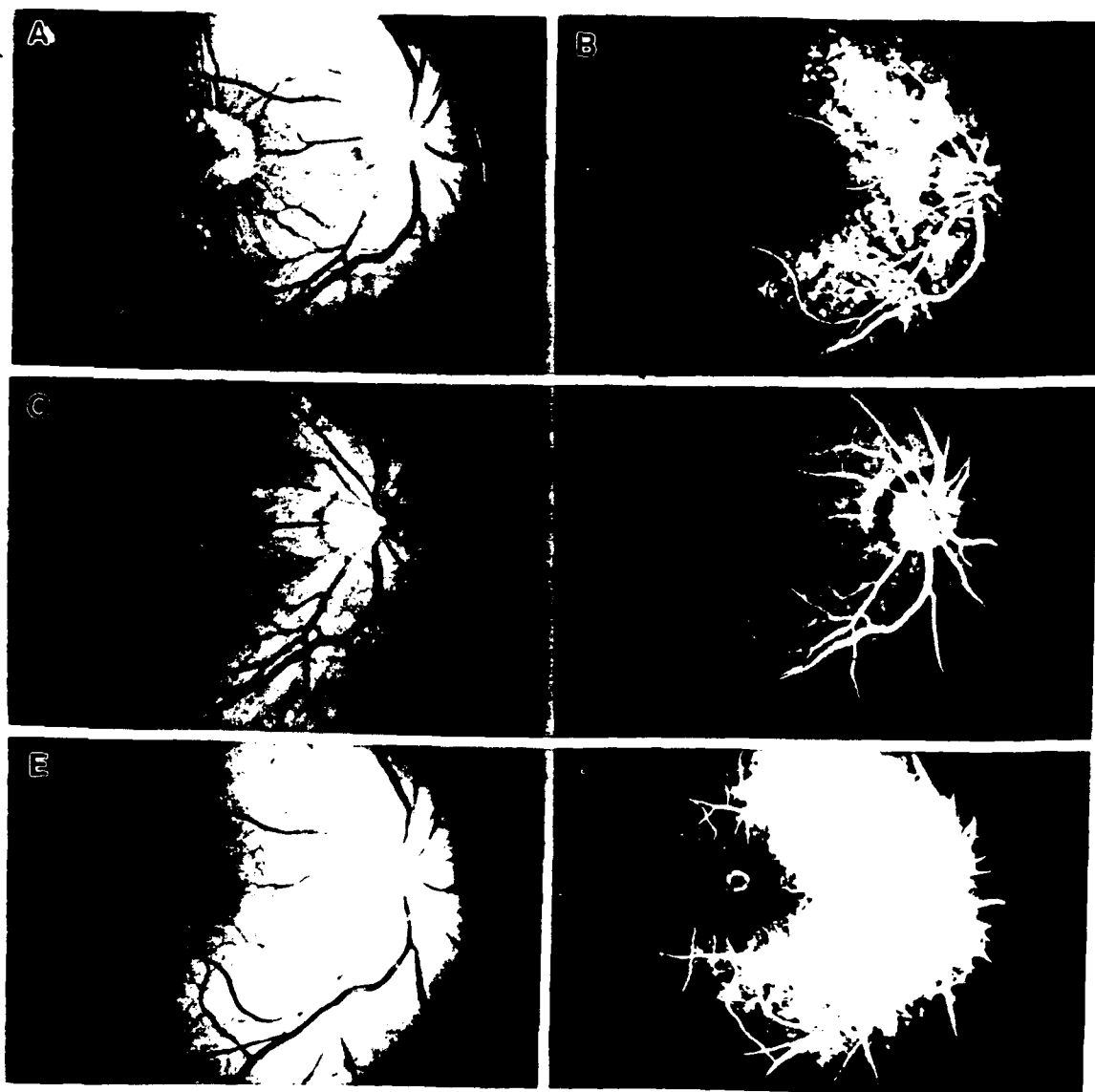


Fig 2.C: Fundus picture and fluorescein angiogram of the right eye of patient #1 at 6 (A, B), 10 (C, D), and 14 (E, F) weeks after laser. See text for description.

AMSLER RECORDING CHART

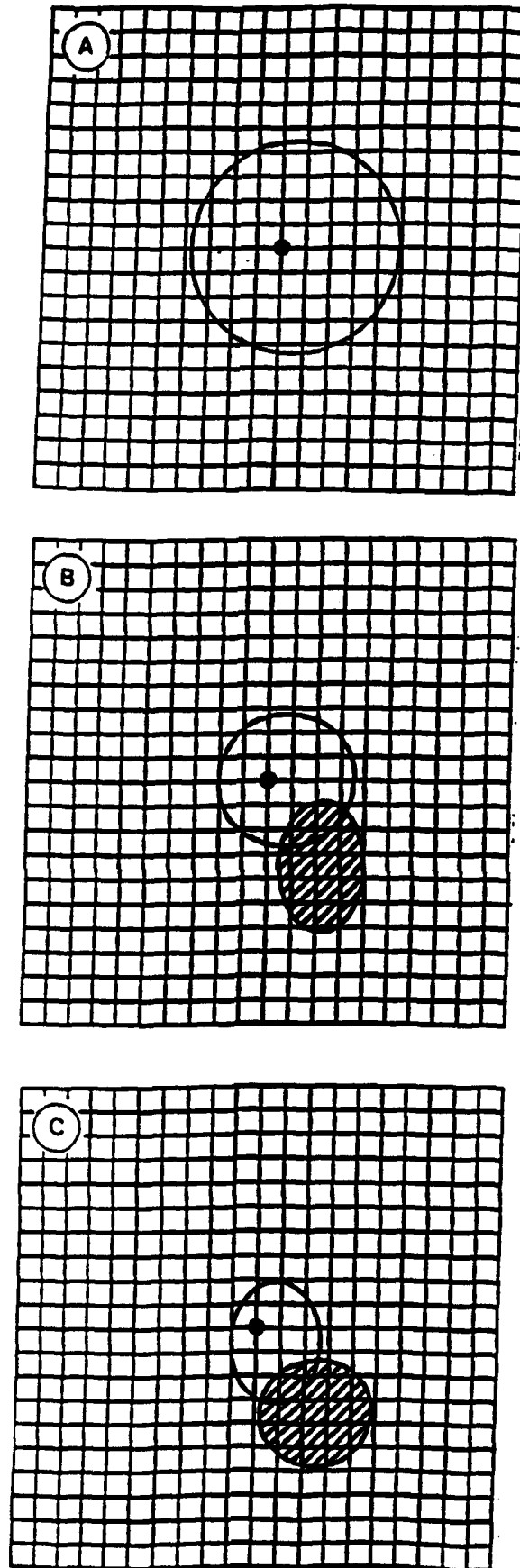


Fig 2.4 Amsler chart of patient #2, at 1 (A), 4 (B), and 10 (C) weeks after injury. See text for description

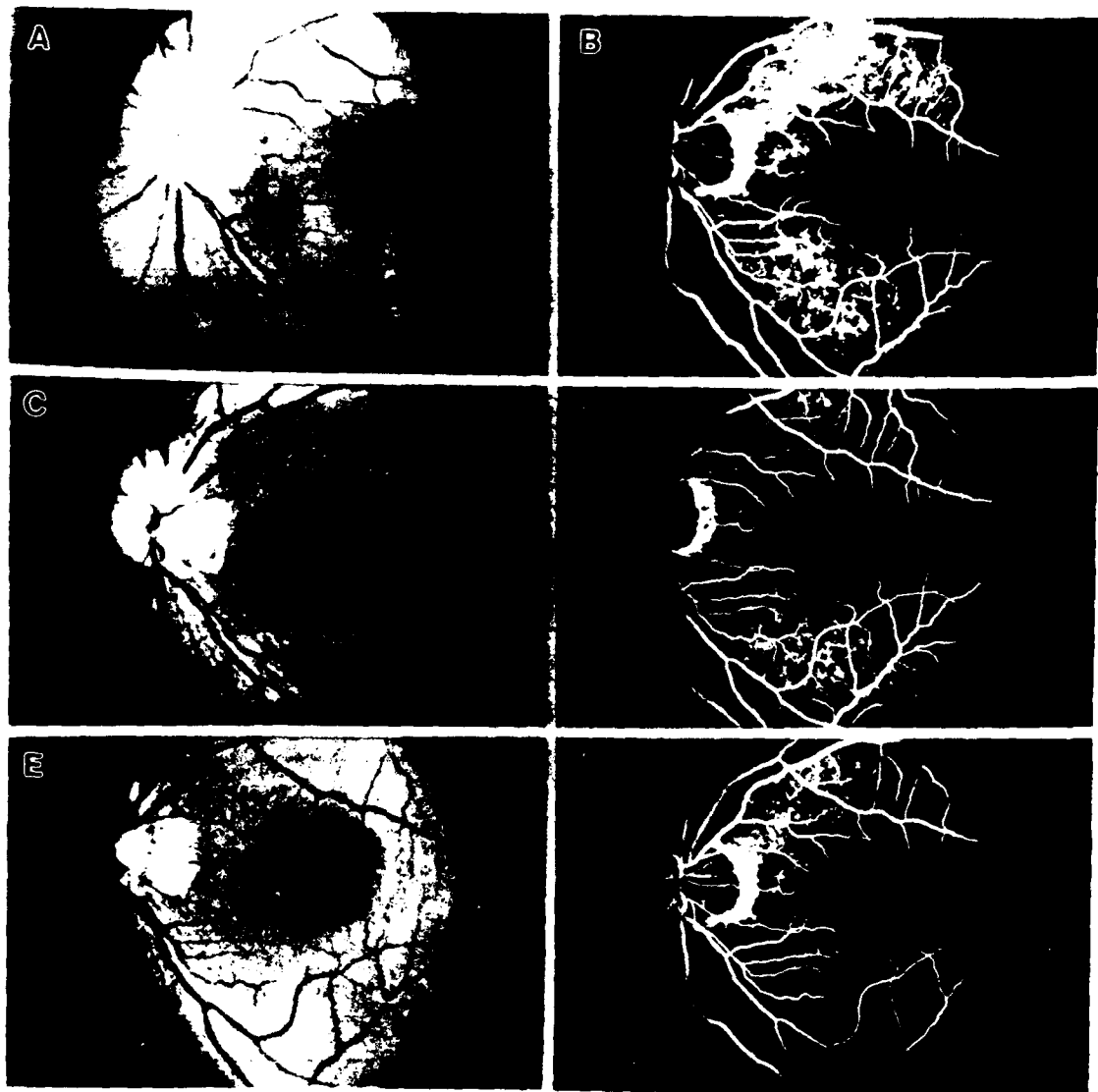


Fig 2.5: Fundus picture and fluorescein angiogram of the left eye of patient #2 at 1 (A,B), 4 (C,D), and 10 (E,F) weeks after injury. See text for description.

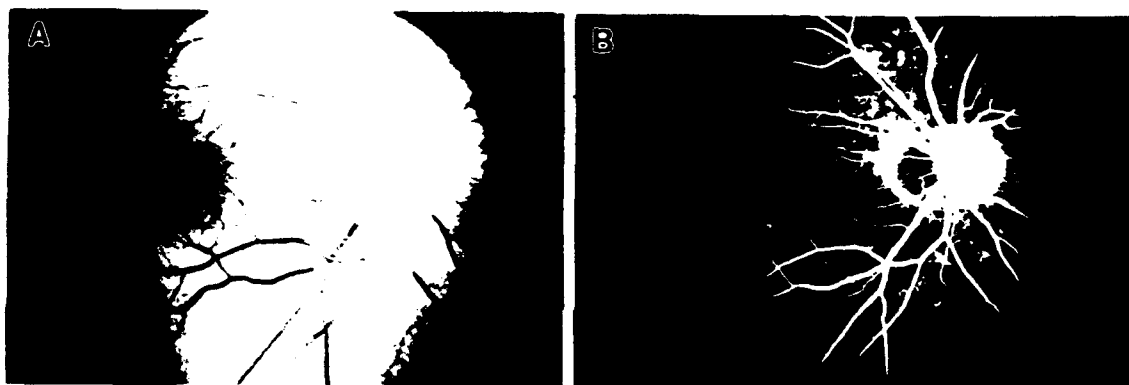


Fig 2.6: Fundus picture and fluorescein angiogram of the right eye of patient #2. See text for description

Chapter 3

Sub-human primate model of non-hemorrhagic retinal laser injury and

Evaluation of the efficacy of high doses of methylprednisolone

3.1 Studies of retinal laser lesions

Clinical and histopathologic changes of laser-induced retinal lesions were well-described¹⁵⁻²³. However, in order to compare the therapeutic effects of different agents on these retinal lesions, we needed to produce experimental retinal laser lesions reproducibly, and to quantify those lesions. In this contract period, we developed a reproducible primate model of laser-induced retinal injury of varying severity. Briefly, using clinical and histopathological criteria we divided retinal laser lesions into four grades: I, II, III, and IV¹⁵. In Grade I lesions, only the retinal pigment epithelial layer was affected. In Grade II lesions, the retinal pigment epithelial layer as well as the outer nuclear layer were affected while in Grade III lesions, the retinal pigment epithelial layer, the outer and inner nuclear layers were all affected. In Grade IV lesions, vitreal hemorrhage was seen in addition to necrosis in all retinal layers.

Previously, there were no quantitative methods established for evaluating the drug effect on retinal laser lesions. In this investigation, we established several morphometric parameters for evaluating these lesions quantitatively. The study of lesions without drug treatment (control study) were presented in section 3.4.1.

3.2 Choice of methylprednisolone (MP)

3.2.1 Effectiveness of MP

Recent advances in pharmacology of neuronal injury suggested that a variety of agents may be beneficial to retinal laser injury. Of the several classes of compounds commonly known to rescue neurons in CNS injury: including calcium antagonist, such as nimodipine¹²; NMDA-receptor antagonist, such as MK-801¹²; and lipid peroxidation inhibitors, such as high doses of methylprednisolone¹³, only high doses of methylprednisolone showed a dramatic and unequivocal beneficial effect on CNS injury in man²⁴. Studies by Hall et al²⁵⁻²⁹ and others established that high doses of methylprednisolone (MP) inhibits lipid peroxidation, which is believed to play an important role in cell membrane disruption and cell death in various injuries, such as spinal cord injury. Recent clinical trial studies showed that high doses of MP was beneficial in acute spinal cord injury in man²⁴.

3.2.2 Pathophysiology consideration

The pathophysiology of spinal cord trauma which comprises of mechanical disruption of neuronal architecture and occlusion of blood supply resulting in ischemia¹³, appears to us to be comparable to that of laser injury, which is also known to cause mechanical/thermal disruption of retinal architecture as well as retinal and choroidal vascular occlusion causing ischemic changes of the retina¹⁹⁻²².

3.2.3 Hypothesis

We hypothesized that in laser-induced retinal lesions, lipid peroxidation aggravates the primary thermal and/or mechanical injury. Hence, MP, a lipid peroxidation inhibitor and a benefactor in the treatment of traumatic spinal cord injury, may ameliorate retinal injury induced by laser. In addition, the anti-inflammatory action of methylprednisolone may also play a role in minimizing the tissue reactions and hence a beneficial effect after laser injury may be achieved (see diagram 2.).

To test our hypothesis, we applied criteria from ophthalmoscopic examination, fundus photography, and fluorescein angiography, histopathology, as well as morphometry to evaluate the efficacy of high dose of methylprednisolone (MP) in laser-induced retinal lesions in monkeys. In addition, we examined three treatment regimens of MP to determine the possible window of treatment. These studies were described in the latter part of this chapter.

3.3 Methods

3.3.1 Characterization of sub-human primate model of non-hemorrhagic retinal laser injury

All animals were treated in accordance with the Association for Research in Vision and Ophthalmology Resolution on the Use of Animals in Research. At least four lesions, each of Grades II and III, were inflicted in comparable areas of the retina in each of the six monkey eyes by a continuous-wave argon (CW Argon) laser (Coherent Medical 920, Palo Alto, CA) with a slit lamp delivery system (Carl Zeiss, Thornwood, NY) and a custom made glass contact lens. Previous studies were conducted to determine the parameters of the continuous-wave Argon (CW Argon) laser required to generate these lesions in the retina consistently using clinical and histopathologic criteria. The energy setting of the laser was determined to be 0.1, 0.25 or 0.7 W for Grades I, II and III respectively. A spot size of 800 micron spot size at the corneal level and 0.1 sec exposure duration were employed. The energy output was monitored using a radiometer (Model 200, Photodyne Inc., Newbury Park, CA). The clinical features of the laser lesions were studied by ophthalmoscopic examination and recorded by fundus photography and fluorescein angiography. The lesions were examined at 3, 10, 20, and up to 90 days after injury. The eyes were enucleated

and fixed in 4% paraformaldehyde and 1% glutaraldehyde, post fixed in Dalton's osmium fixative, dehydrated in alcohol, and embedded in epoxy resin. One micron serial sections were cut until the center of the lesion, which was defined by the largest morphometric indices described below, was reached and studied by light microscopy.

Morphometric indices based on histopathologic features were used to quantify the effectiveness of drug treatment. We measured the width of the disrupted photoreceptor layers, representing the extent of the total loss (absence) of photoreceptor cells, and the width of depigmented RPE, representing the extent of damage to the RPE (see diagrams). For Grade II lesions, 4 lesions each for 3, 10, and 20 days after the injury were examined. For Grade III lesions, 15 control lesions from 4 eyes of 2 animals at 3 (4 lesions), 10 (4 lesions), 20 (4 lesions), and 90 (4 lesions) days after injury were examined.

3.3.2 Efficacy of methylprednisolone in non-hemorrhagic retinal laser injury

Fifteen Grade III lesions which showed damage extending from choroidal capillaries, RPE, outer nuclear to inner nuclear layers, and with no retinal or choroidal hemorrhages, from four eyes of three Cynomolgus monkeys were examined in the treatment groups. Ten days after laser injury was selected for evaluating the efficacy of methylprednisolone. For the drug treatment studies all retinal lesions were followed clinically and eyes were enucleated 10 days after injury. The retina was fixed in 4% paraformaldehyde and 1% glutaraldehyde, postfixed in Dalton's osmium fixative, dehydrated in alcohol and embedded in epoxy resin. One-micron serial sections were cut until the center of the lesion, defined as the widest diameter of the lesion determined by morphometric measurements, was reached.

3.3.2.1 Administration of methylprednisolone

A swivel tethering system (Alice King Chatham Medical, Los Angeles, CA) and a syringe pump (Model 355, Sage Instrument, Boston, MA) were used for continuous intravenous infusion of methylprednisolone (Upjohn, Kalamazoo, MI) in saline in the animals. The doses used were comparable to those of the Second National Acute Spinal Cord Injury²⁴. Methylprednisolone was administered at three different regimens (see diagram 4):

Treatment I: An initial dose of 30 mg/kg was given intravenously 24 hours before laser injury. Continuous infusion of methylprednisolone at 5.4 mg/kg/hr began 1 hour after the first injection, and continued for 3 days after laser injury for a total treatment of 4 days. A total of 7 lesions from two eyes of two animals were studied.

Treatment II: An initial dose of 30 mg/kg of methylprednisolone was given intravenously to one animal immediately after laser injury to the retina. Continuous infusion of methylprednisolone at 5.4 mg/kg/hr began 1 hour after laser and continued for 4 days. Four lesions from one eye were studied.

Treatment III: A loading dose of 30 mg/kg of methylprednisolone was given intravenously immediately after laser injury. Continuous infusion of methylprednisolone at 5.4 mg/kg/hr began 1 hour after the laser injury and continued for 8 hours after laser injury. Four lesions from one eye of a single monkey were studied.

3.3.2.2 Morphometric evaluation

The width of the disrupted photoreceptor layers and the width of the depigmented RPE of the retinal lesions were measured (see diagram 5). Since all laser lesions were less than 600 microns in diameter, the number of remaining paralesional photoreceptor nuclei within a 250 micron radius from the center of the lesion was counted. This value was compared with the number of photoreceptor nuclei from the same section taken from areas unaffected by the laser burn and reported as the percentage of the residual photoreceptor cells.

3.4 Results

3.4.1 Characterization of sub-human primate model of non-hemorrhagic retinal laser injury without medication

3.4.1.1 Histopathologic features of Grades II and III lesions in normal monkeys without medication

Figure 3.1 showed sections of Grade II retinal lesions from 3 days up to 20 days after laser treatment. At 3 days (A) after laser injury, choriocapillaries showed partial narrowing. Retinal pigment epithelium exhibited total necrosis with macrophages at the edge of the lesion. The outer segments showed coagulative necrosis and the inner segment showed focal densification. The outer nuclear layer had total coagulative necrosis with pyknotic nuclei. The outer plexiform layers were vacuolated. The inner nuclear layers and inner retina were unremarkable. At 10 days (B) after the injury, the choriocapillaries were patent. The RPE exhibited regeneration (single layer). A few pigment-laden macrophages in the subretinal space were noted. Outer segments and inner segments were totally absent. There was total loss of outer nuclear layer at the center of the lesion. The inner retina appeared to be unremarkable. At 20 days (C) after injury, the choriocapillaries were opened. RPE showed proliferative reaction focally. There was a decrease in the number of macrophages but they could still be seen in the subretinal space. At the center of the lesions there was total absence of outer nuclear layer, and pyknotic nuclei were still noted at the periphery of the lesion. Edema of the outer plexiform layer subsided. The inner layer appeared unremarkable.

Figure 3.2 showed Grade III retinal lesions from 3 days up to 90 days after laser insult. At 3 days (A) after the injury, the width of the lesion appeared to be larger than Grade II lesions. The choriocapillaries were occluded. RPE was necrotic. Macrophages were noted at the edge of the

lesion. Both outer and inner segments showed coagulative necrosis. There was total loss of photoreceptor cells at the center of the lesion and pyknotic nuclei were noted at the periphery. The inner nuclear layer showed pyknotic nuclei with coagulated necrosis and edema. At 10 days (B) after laser injury, the choriocapillaries remained occluded. There was active RPE proliferation. Pigment-laden macrophages were noted. There was total loss of outer nuclear layer at the center of the lesion. Macrophagic cells were noted in the inner retina. The inner nuclear layer showed focal necrosis and scattered pyknotic nuclei were noted. At 20 days (C) after the injury the choriocapillaris was partially open but appeared to be narrowed. Multi-layered RPE cells were noted with macrophages in the subretinal space. There was total loss of photoreceptor cells. In the inner retina, vacuolization and edema were noted. There was also loss of inner nuclei and pyknotic nuclei. At 90 days, the choriocapillaries (D) were partially opened. Mild RPE proliferation was noted. The photoreceptor cells were totally absent at the center of the lesion. A few macrophages were observed to aggregate in subretinal space as well as in the inner nuclear layer. Also seen were some nuclei from the inner nuclear layer which slipped down into the gap left by the outer nuclear layer. The inner plexiform layer was unremarkable.

3.4.1.2 Morphometry of Grades II and III control lesions

Figure 3.3 showed that measurements of the outer nuclear layer gap and the retinal pigment epithelial depigmentation in Grade II lesions were dependent on the time after injury. Both parameters showed a sharp decrease from 3 days to 10 days and remained unchanged from 10 to 20 days after laser injury.

Figure 3.4 depicts the morphometric changes of the control Grade III retinal laser lesions with time ranging from 3 to 90 days after laser exposure. The initial width of the depigmented RPE in the retinal lesions 3 days after exposure was $637 \pm 49 \text{ } \mu\text{m}$ ($n=5$) and showed a mild decrease from 3 days to 10 days (not statistically significant). However, a total reduction of 22% from day 3 to day 90 ($505 \pm 35 \text{ } \mu\text{m}$, $n=3$) was statistically significant ($P < 0.02$, Fig 3.4A). At 3 days after injury, the outer nuclear layer gap (Fig 3.4B) representing the total absence of photoreceptor cells at the center of the lesion was $378 \pm 10 \text{ } \mu\text{m}$ ($n=4$), but was reduced by 47% in the first 20 days to $183 \pm 32 \text{ } \mu\text{m}$ ($n=4$) and further narrowed to $101 \pm 6 \text{ } \mu\text{m}$ ($n=3$) 90 days after injury. The remaining photoreceptor cells in the affected area (500 μm width) were expressed as a percentage of the normal population of photoreceptors and were only 8% of normal at 3 days (Fig 3.4C). However, at 20 days after injury, the photoreceptor cell counts in the affected area were increased to 58% and remained unchanged at approximately 50% until 90 days.

Figure 3.5 showed the relationship between the laser energy and the outer nuclear gap, and the retinal pigment epithelium depigmentation measured at 10 days after injury. There was linear relationship between the energy applied and the parameters measured: namely the outer

layer gap and the retinal pigment epithelium depigmentation.

3.4.2 Efficacy of methylprednisolone in non-hemorrhagic retinal laser injury

The efficacy of methylprednisolone was tested in Grade III retinal lesions by clinical, morphologic, and morphometric retina.

3.4.2.1 Clinical features

Figures 3.6 and 3.7 illustrate the ophthalmoscopic and fluorescein angiographic appearance of the retinal laser lesions in the control and the three treatment regimens groups at 3 days (Fig. 3.6), and 10 days (Fig. 3.7) after laser. Three days after injury, the control retinal lesions had a dense whitish center with a grayish ring at the periphery (Fig 3.6A). Fluorescein angiogram showed extensive fluorescein leakage (Fig 3.6B). In contrast, the retinal lesions treated by Regimen I at three days after laser exhibited a smaller spot size and a mild grayish appearance without a dense whitish center (Fig 3.6C). These lesions also leaked fluorescein diffusely (Fig 3.6D). The retinal lesions treated by Regimen II had a whitish center and grayish ring (Fig 3.6E), but the whitish center appeared to be smaller and comparable leakage of fluorescein was noted (Fig 3.6F). The retinal lesions treated by Regimen III were comparable to the control retinal lesions showing a whitish center with a grayish ring ophthalmoscopically (Fig 3.6G) and leaked fluorescein diffusely (Fig 3.6H).

Ten days after laser injury the control retinal lesions became grayish with a diminishing whitish center with an irregular edge (Fig 3.7A). Fluorescein angiogram showed only mild hyperfluorescence at the periphery of the lesion with a hypofluorescent center (Fig 3.7B). The retinal laser lesions treated by Regimen I showed faint grayish lesions with irregular outline (Fig 3.7C) and exhibited mild staining in the central area of the lesions with a hypofluorescent periphery (Fig 3.7D). The retinal laser lesions treated by Regimen II revealed relatively faint grayish color with small grayish-brown centers (Fig 3.7E). Fluorescein angiography showed staining in the periphery of the lesion with a hypofluorescent center (Fig 3.7F). The retinal laser lesions treated by Regimen III were grayish with a grayish-brown center (Fig 3.7G). Fluorescein angiography showed hyperfluorescence in the periphery with a hypofluorescent center (Fig 3.7H), which was smaller but comparable to the control lesions.

3.4.2.2 Histopathologic Studies

Figure 3.8 shows the histopathologic changes 10 days after laser exposure of the control retinal lesions (Fig 3.8A) and those treated with regimens I, II, and III (Fig 3.8 B,C,D.).

Control Group: Ten days after the laser-injury in the control lesions (Fig 3.8A), the choriocapillaris and the medium-sized choroidal vessels (O) at the center of the control lesions

were occluded and the lumina of the choriocapillaris at the periphery of the lesion were narrow. Bruch's membrane appeared intact. At the periphery of the lesion, the RPE (R) proliferated to form two to three layers of flattened cells over Bruch's membrane. Aggregates of pigment-laden macrophages (M) migrated into the subretinal space. Photoreceptor nuclei, the inner and outer segments, the external limiting membrane and outer plexiform layer were completely absent at the center of the lesion (between arrows), while at the periphery of the lesion the inner and outer segments were shortened. The outer nuclear layer showed a few remaining pyknotic nuclei (arrow heads) at the edges of the lesion. The inner nuclear layer was disrupted at the center of the lesion and approximated the subretinal space. Pigment-laden macrophages and proliferated RPE invaded into the inner retinal layers. The inner plexiform layer was mildly vacuolated. The retinal ganglion cells and the nerve fiber layer remained unremarkable.

Treatment Regimen I: In contrast, in the lesions treated with Regimen I (Fig 3.8B), the choriocapillaris and deeper choroidal vessels were patent (V). Bruch's membrane appeared intact. The depigmented RPE cells (R) proliferated into one to two layers covering Bruch's membrane. Few pigment-laden macrophages (M) migrated into subretinal space. The nuclei and the inner and outer segments of the photoreceptors were absent at the center of the lesion (between arrows) but the outer limiting membrane was re-formed. The outer nuclear layer was largely replaced with Muller cell processes. A few pyknotic nuclei (arrow heads) were also noted at the edge of the lesion. The outer plexiform layer at the periphery of the lesion showed loss of cone pedicles and rod spherules and was invaded by a few macrophages. The outer portion of the inner nuclear layer exhibited a few pyknotic nuclei. The inner plexiform layer, ganglion cell layer, nerve fiber layer and inner limiting membrane appeared normal.

Treatment Regimen II: In the retinal lesions treated with Regimen II (Fig 3.8C) the choriocapillaris was occluded at the central part of the lesion and medium-sized choroidal vessels were occasionally occluded (O). Bruch's membrane appeared intact and the RPE (R) proliferated into two to three layers. A layer of pigment-laden macrophages (M) was seen anteriorly to the proliferated depigmented RPE cells. The nuclei and outer and inner segments of photoreceptor cells were absent (between arrows) at the center of the lesion but the outer limiting membrane was re-formed. The outer nuclear layer was replaced by Muller cells processes. At the edge of the lesion a few pyknotic photoreceptor nuclei were present and the outer plexiform layer showed loss of cone pedicles and rod spherules. A few pyknotic cells (arrow heads) were noted at the outer portion of the inner nuclear layer. Pigment-laden macrophages invaded both the outer plexiform layer and the inner nuclear layer, and were occasionally found in the ganglion cell layer. The nerve fiber layer and inner limiting membrane appeared unremarkable.

Treatment Regimen III: In the retinal lesions treated with Regimen III (Fig 3.8D), the choriocapillaris (O) was occluded at the center of the lesion and the medium-sized choroidal

vessels were patent. Bruch's membrane appeared intact. The retinal pigment epithelium (R) showed placoid proliferation into two to three layers. The nuclei and inner and outer segments of the photoreceptors had completely disappeared at the center of the lesion (between arrows), and aggregates of the pigment-laden macrophages (M) were present in the subretinal space. The outer plexiform layer, inner nuclear layer, and inner plexiform layer were focally disrupted and infiltrated by pigment-laden macrophages. A few migrated pigment-laden macrophages had wandered into the ganglion cell and nerve fiber layers.

3.4.2.3 Morphometric Measurements

Figure 3.9 shows the effect of different treatment regimens on laser-induced lesions on the morphometric parameters measured 10 days after the initial insult. Measurements of all three parameters, including the width of depigmented RPE (Fig 3.9A), the outer nuclear layer gap (Fig 3.9B), and the percentage of remaining photoreceptor nuclei (Fig 3.9C), showed a beneficial effect of methylprednisolone treatment with Regimen I and II, but not with Regimen III. In all three parameters, Treatment Regimen I appeared to be more beneficial; however, there was no statistically significant difference between Treatment Regimen I and II in all three measurements. In the control group, RPE depigmentation was 574 ± 30 μ m while methylprednisolone Treatment Regimen I reduced the RPE depigmentation by 30% (400 ± 49 μ m $P < 0.01$), and Treatment Regimen II reduced by 27% to 416 ± 56 μ m ($P < 0.02$) and Treatment Regimen III showed no significant difference (532 ± 43 μ m) (Fig 3.9A). Similarly, methylprednisolone Treatment Regimen I reduced the outer nuclear layer gap by 53% (247 ± 23 μ m to 107 ± 44 μ m, $P < 0.01$), whereas under Treatment Regimen II, the outer nuclear layer gap was reduced by 32% to 160 ± 17 μ m ($P < 0.02$). Treatment Regimen III showed no change (246 ± 12 μ m, $P > 0.8$) (Fig 3.9B). Study of the remaining photoreceptor cells in the affected area (Fig 3.9C), showed that Treatment Regimen I had twice the number of photoreceptor cells compared with the controls ($68 \pm 12\%$ vs $32 \pm 6\%$, $P < 0.01$). Treatment Regimen II appeared less effective but significantly more photoreceptor cells remained in the lesion area ($44 \pm 5\%$, $P < 0.02$ vs. control). Treatment III yielded no difference compared with the controls ($34 \pm 8\%$, $P > 0.8$).

3.5 Comment

3.5.1 Characterization of the subhuman primate model

We were able to document the histopathological features of 2 grades of retinal lesions induced by laser. The two quantitative parameters proposed, namely the outer nuclear layer gap and the width of retinal pigment epithelial depigmentation appeared to be sufficient for the evaluation of drug efficacy as demonstrated by the linear dependency of the parameters on the intensity of the laser.

Sliding of photoreceptor cells into the lesional area after laser injury has previously been

observed but has not been quantitated. With the measurement of the outer nuclear layer gap after laser injury and/or the percentage of photoreceptor cells remaining in the lesion area, we were able to demonstrate quantitatively the movement of photoreceptor cells into the lesion area in the control group without methylprednisolone-treatment. In Grade II lesion, the gap was reduced as much as 47% from day 3 to day 20 after injury and reduced to 74% at 90 days. Similar recovery was observed in Grade III lesions. This dramatic repair may explain the remarkable recovery of vision in patients after laser injury over the period of months. It will be important to know if this repair is due to the active sliding movement of photoreceptor cells or by passive push and pull by other elements such as Muller cells of the retina.

3.5.2 Effects of methylprednisolone on the retinal lesions

3.5.2.1 Efficacy

This series of experiments represents the first attempt of a controlled study to evaluate the efficacy of three different regimens of high doses of methylprednisolone treatment on retinal injury induced by Argon laser with clinical, histopathologic, and morphometric criteria. Under these three criteria, treatments with Regimens I and II showed remarkable beneficial effects on laser-induced retinal injury. Clinically and histopathologically, treatment with Regimen III also showed improvement; but morphometrically, there was no significant difference as compared to control. The fundus pictures of animals given Regimen I, II, and III suggested a rapid reformation of the blood-retinal barrier, decrease in fluorescein leakage, and less edema. Histopathologically, under all Regimens, the retina showed improved patency of choroidal vessels, rapid and active proliferation of RPE on Bruch's membrane, more surviving photoreceptors in the lesioned area, and rapid reforming of the outer limiting membrane. Morphometric criteria suggested better preservation of RPE, and more photoreceptor cells in the lesion area when Regimens I or II were given.

3.5.2.2 Clinical Pathological Correlation

Our clinical observations of the control and treatment lesions at 10 days after laser insult showed remarkable correlation with their corresponding histopathologic features. In the control group, infiltration of pigment-laden macrophages into the central portion of the lesion observed histopathologically was consistent with a grayish-brown appearance in the fundus photography and a hypofluorescent center in fluorescein angiography. Similarly, active leakage of fluid from RPE at the periphery of the lesion noted was consistent with the whitish edges of lesions in fundus picture and mild hyperfluorescence at the edges of the lesions in fluorescein angiography. Under Regimen I, limited infiltration of pigment-laden macrophages into the central area of the lesion, and

accumulation of pigment-laden macrophages at the periphery of the lesion gave rise to whitish lesions in fundus photography and a hypofluorescence center with a hyperfluorescence edge in fluorescein angiography. Likewise, with Regimens II and III, infiltration of pigment-laden macrophages into the center of the lesion caused a grayish center with whitish edges on fundus examination and a hypofluorescence center with mild hyperfluorescence edges in fluorescein angiography.

3.5.2.3 Dose and window of treatment

In contrast to most ophthalmic uses of corticosteroids, we employed a high dose of methylprednisolone (30 mg/kg intravenous bolus injection followed by 5.4 mg/kg/hr). This dosage was chosen because of experimental data suggesting its efficacy in various animal models of the central nervous system injuries and its proven efficacy in the Second National Clinical Trial Study of Acute Spinal Cord Injury²⁴. It has been also reported that doses lower or higher than the recommended dose were not effective^{26,30,31}. Instead of administering for 24 hours as the published clinical trial study, we arbitrarily prolonged the administration to 4 days after laser injury to inhibit possible other degenerative processes. Since we demonstrated that 8 hours of treatment showed only limited effects and was not as effective as 4 days, it is very likely that the effective period of treatment might be between 8 hours and 4 days. Further experiments are needed to determine the window of treatment and the effective period of treatment.

3.5.2.4 Effects on choroidal vessels

At the center of the control lesions, medium-sized choroidal vessels and choriocapillaries were occluded. In all treated lesions, the choriocapillaries and choroidal vessels showed different degrees of beneficial effects. Treatment Regimen I was the most effective one, and the choriocapillaries and choroidal vessels in those lesions were remarkably patent while lesions in Treatment regimens II and III, showed some occlusion of mid-sized choroidal vessels and choriocapillaries. Hence, the effectiveness of the treatment appeared to be partially related to the patency of choroidal vessels. Since high doses of steroids are known to have dilating and protective effects on microcirculation, the patency of choroidal vasculature in the treated groups may contribute to diminished ischemic damage of the retinal tissues, and hence, better outcome. This observation is also consistent with the hypothesis that retinal laser injury may have an ischemic component.

3.5.2.5 Effects on RPE

Functional integrity of the RPE has been proposed to be vital for effective photoreceptors. Both our clinical and histopathologic features in the treated retinas suggested a rapid re-

establishment of the blood-retinal barrier at the RPE in the treated groups. It appears that methylprednisolone expedites the rebuilding of the blood-retinal barrier with restoration of RPE functions, thereby limiting other secondary injurious changes to the photoreceptor cells. However, in the 8 hours treatment Regimen (Treatment Regimen III), while remarkable RPE regeneration was noted, there were no ameliorative effects on injury to the photoreceptor cells. Other factors might play a role in the reparative process.

3.5.2.6 Effects on outer limiting membrane

Histopathologically, in all treated groups, there was a rapid reforming of the outer limiting membrane by the Muller cells. This observation suggested that methylprednisolone might also act on Muller cells. However, this effect on Muller cells may not have a major role in photoreceptor rescue since Regimen III showed similar reformation of the outer limiting membrane but limited overall beneficial effect.

3.5.2.7 Effects on photoreceptors

Morphometric indices suggested more photoreceptor cells in the retinas given methylprednisolone in Regimens I & II. In the control lesions, there is movement of adjacent photoreceptor cells into the center of the lesion after injury. This beneficial effect of methylprednisolone may be due to (1) the preservation of photoreceptor cells, or (2) the promotion of the repair of photoreceptor cells. Further studies are needed to examine these possibilities.

3.5.2.8 Mechanisms of methylprednisolone

The mechanisms of the action of methylprednisolone in CNS and spinal cord injuries may be multifaceted and included: (a) to reduce edema, (b) to moderate anti-inflammatory reaction, (c) to maintain microvascular integrity, (d) to reduce potassium loss, (e) to attenuate oxygen free radical reactions with the reduction of lipid peroxidation, (f) to enhance sodium and potassium ATPase activity, (g) to cause hyperpolarization of neuron-resting membrane potentials, and (h) to accelerate impulse conduction along the axons²⁴. However, inhibition of lipid peroxidation is believed to be the major factor²⁴⁻³¹. Similarly, MP may work in retinal laser injury through some of those mechanisms with inhibiting lipid peroxidation as a major factor.

It has been proposed that laser-induced retinal injuries were caused by three basic mechanisms, namely, photochemical, mechanical, and photodisruption; but there is limited evidence of lipid peroxidation in the retina after laser. Photochemical injury by laser has been suggested by the observation that ophthalmologists involved in laser therapy had lower sensitivity to blue light. Cai et al⁷ recently reported that Argon laser injury to the rabbit retina caused increased levels of malondialdehyde (MDA), a product of these lipid peroxidation, in the retina at

24 hours after the initial insult. The authors went on to suggest that lipid peroxidation products are probably due to photochemical injury by laser to the retina. Hence, it is possible that methylprednisolone may inhibit the formation of toxic products from lipid peroxidation by photochemical injury to the retina by laser or other mechanisms.

3.5.2.9 Summary

In summary, this report demonstrates that we established a reproducible primate model for evaluating drug efficacies for retinal laser injury. In addition, we demonstrated that choroidal vessel alterations and the disruption of the blood-retinal barrier as well as photoreceptor and Muller cell responses after injury may be modified with high doses of methylprednisolone. These findings suggested that high doses of methylprednisolone for an appropriate period might be beneficial to the patients after laser injury.

ADMINISTRATION

Dose: 30 mg/kg Bolus; I.V.
5.4 mg/kg/hr Continuous I.V.; started 1 hour after bolus injection

Regimen

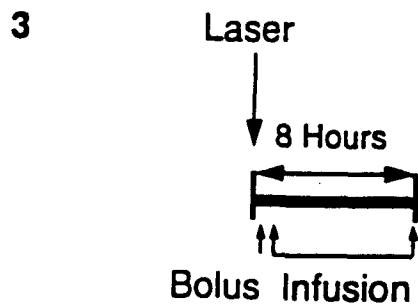
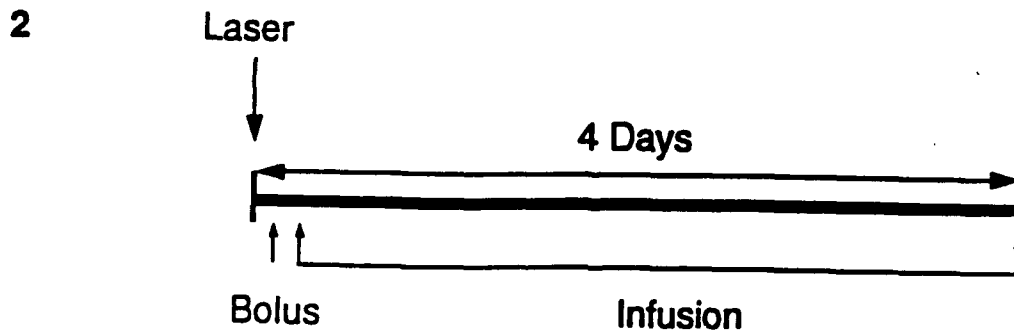
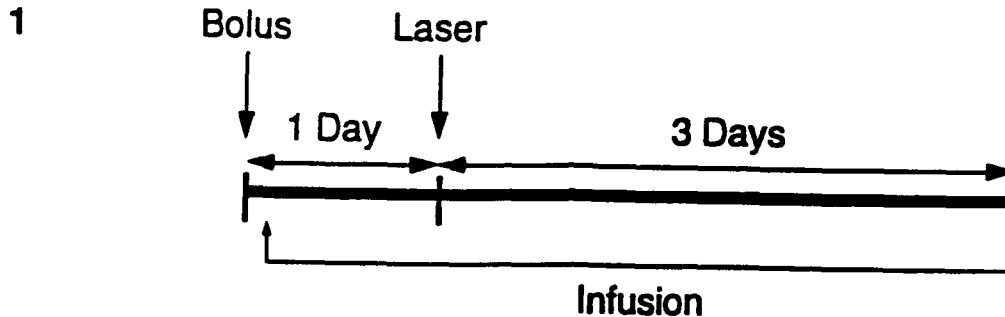


Diagram 4: Schedule of administering methylprednisolone



Diagram 5: Illustration of morphometric indice for laser lesion. Outer nuclear layer (ONL) gap (A) and depigmentation width of retinal pigmented epithelium (RPE) (B) were measured as shown.

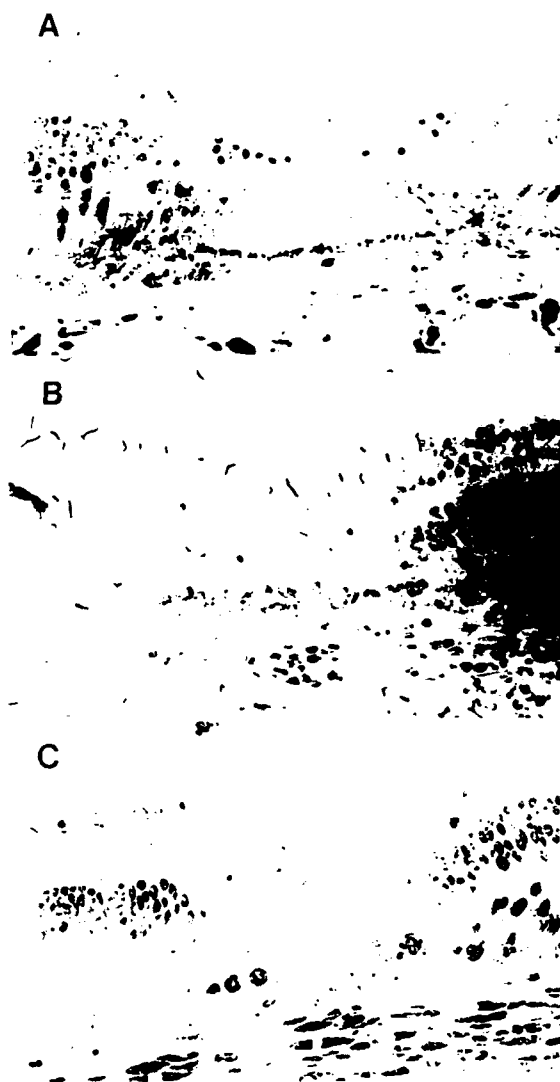


Fig 3.1: Histopathologic changes of Grade II laser lesions at 3 (A), 10 (B), and 20 (C) days after injury in primate. For description, see text 3.4.1



Fig 3.2: Histopathologic changes of Grade III laser lesions at 3 (A), 10 (B), 20 (C), and 90 (D) days after injury in primate. For description, see text 3.4.1

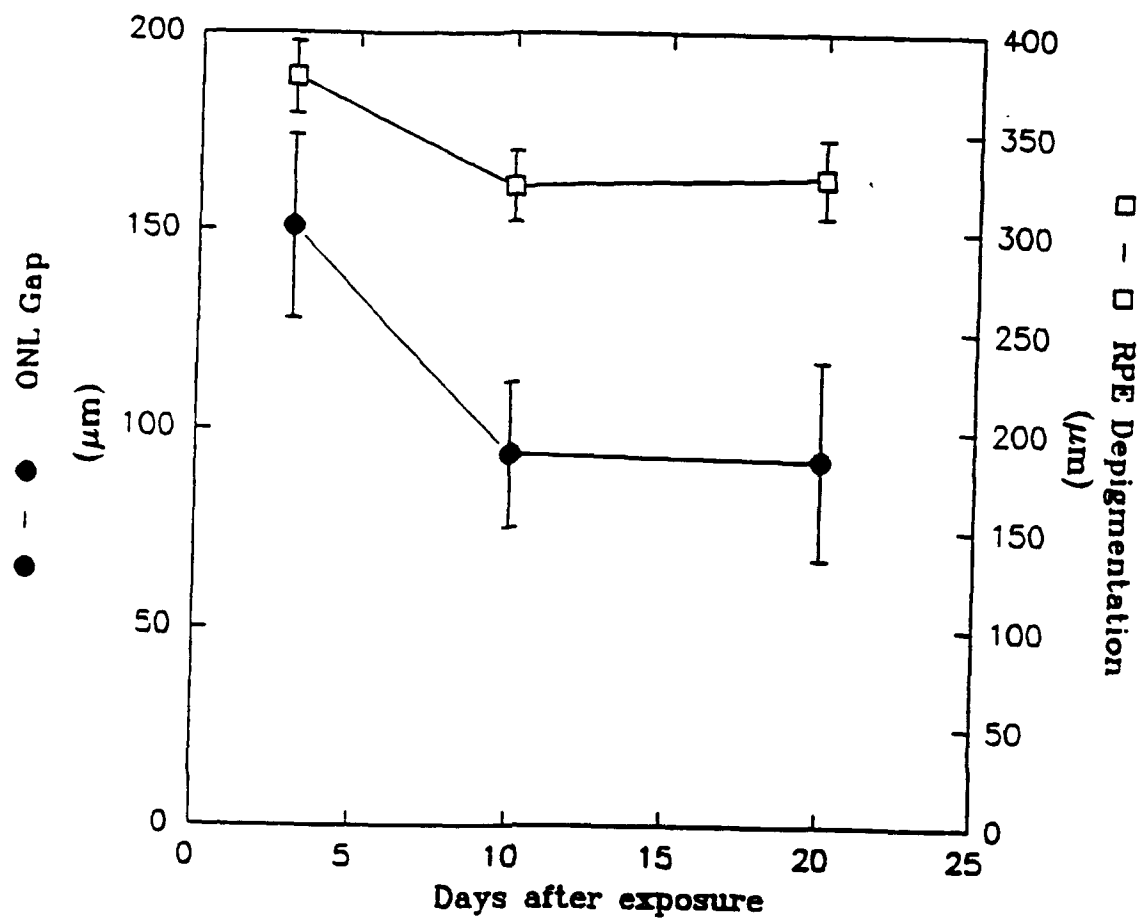


Fig 3.3: Morphometric changes of the control Grade II lesions according to time after injury.

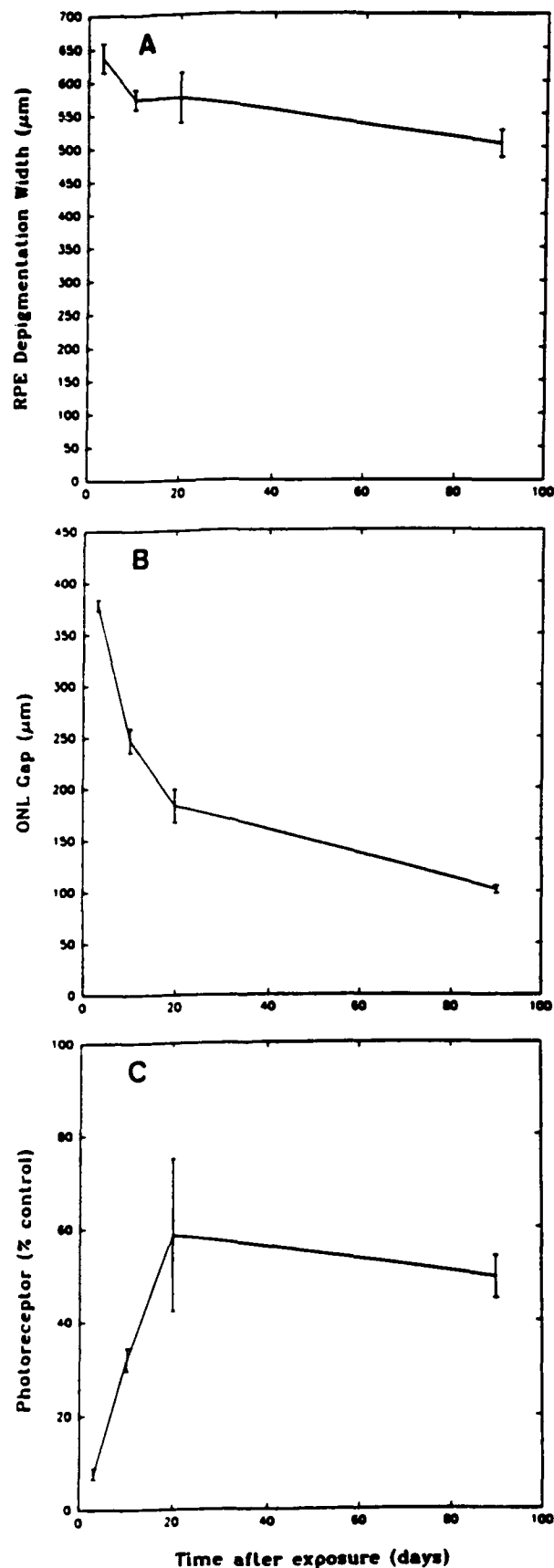


Fig 3.4 Morphometric changes of the control Grade III laser lesions with time after exposures. **A.** Change of the width of the depigmented RPE region according to time after exposure. **B.** Change of the ONL gap according to time after exposure. **C.** Change of the percentage of remaining photoreceptor cells in the affected area according to time after exposure.

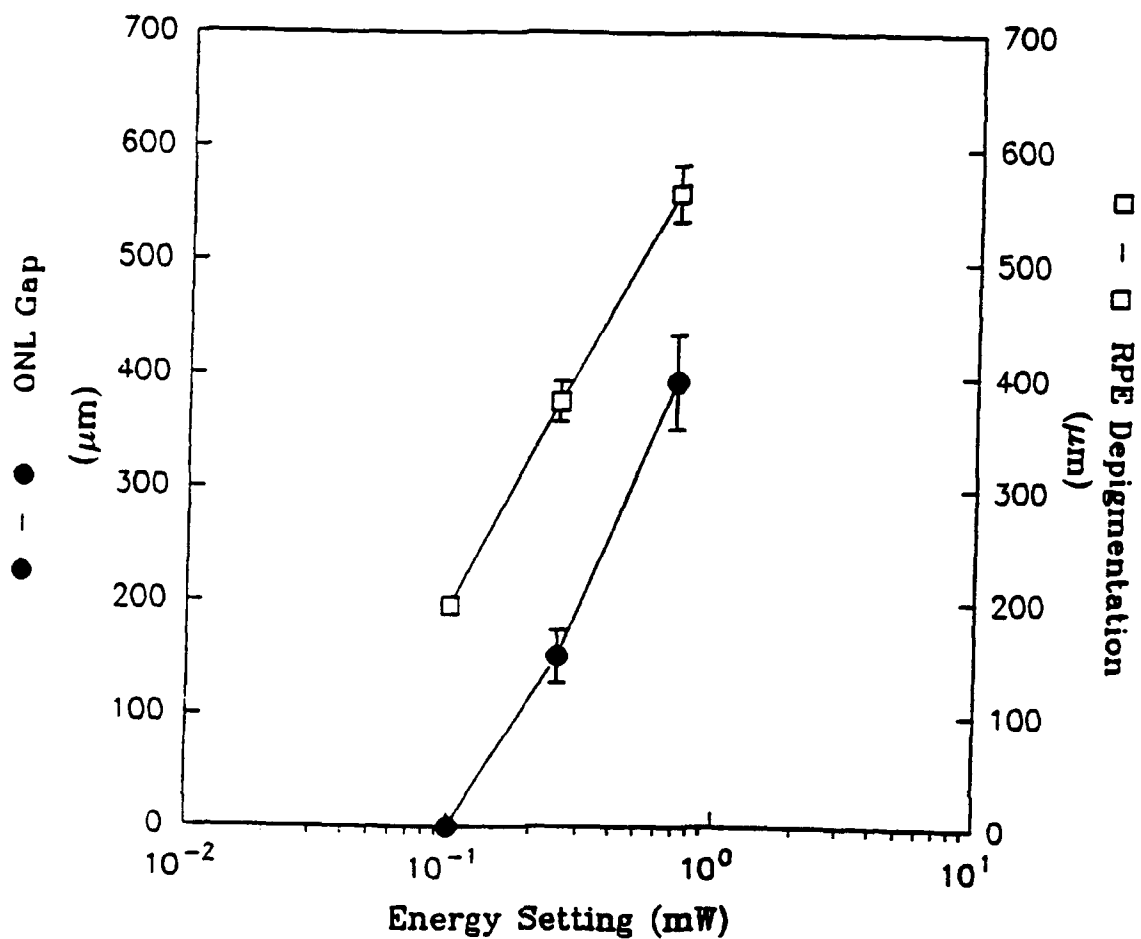


Fig 3.5: Linear dependency of morphometric indice on the energy setting of the Argon laser.

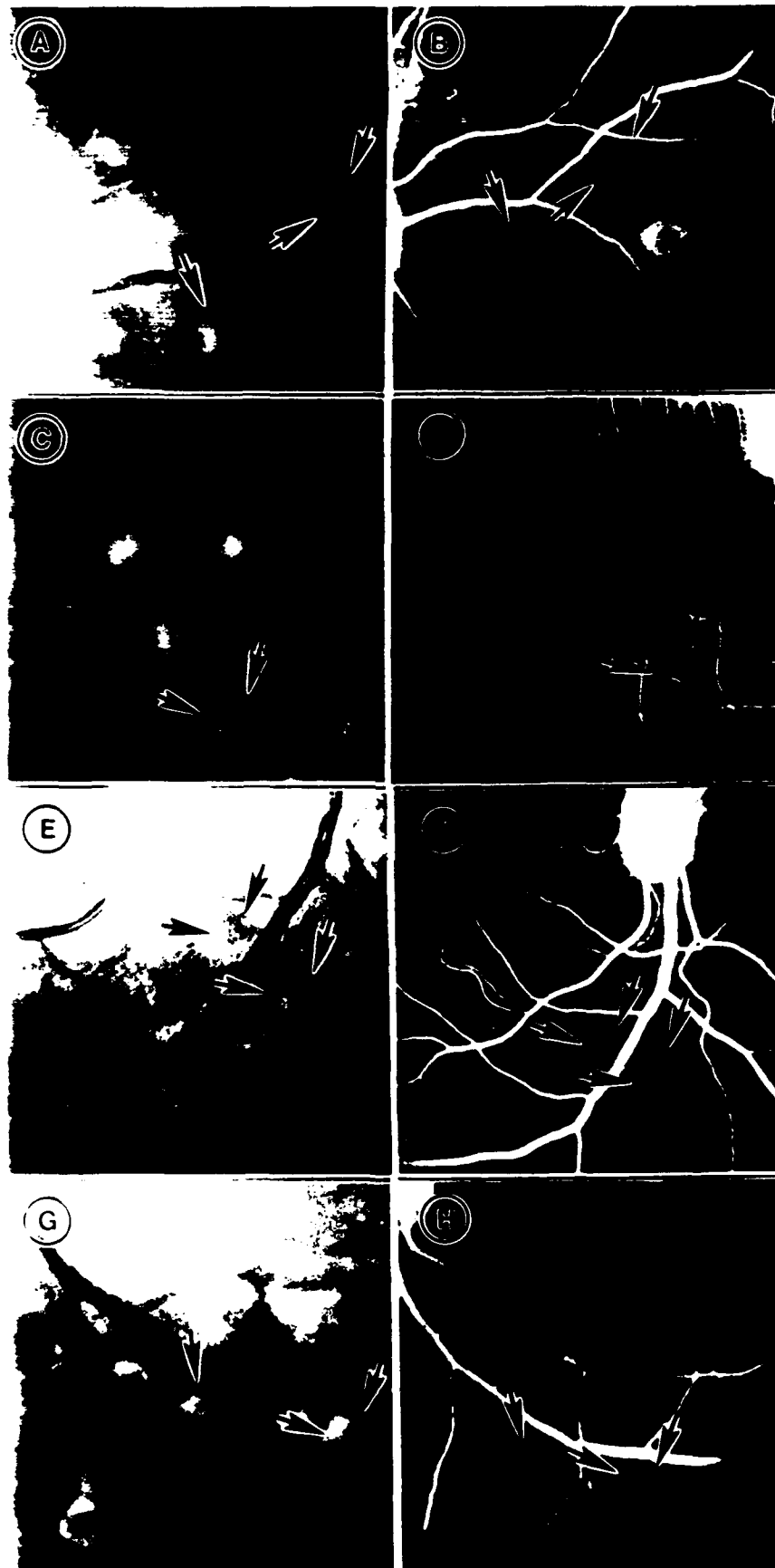


Fig 3.6: Ophthalmoscopic and fluorescein angiographic appearance of Grade III (arrows) lesions in the control (A, B), Treatment Regimen I (C, D), Treatment Regimen II (E, F), and Treatment Regimen III (G, H) groups at 3 days after laser exposure. Retinal lesions of varying severity (Grade II and Grade III) were inflicted by CW Argon laser in the posterior retina of Cynomolgus monkeys and only those of Grade III (arrows) were illustrated. For description, see text 3.4.2.1.

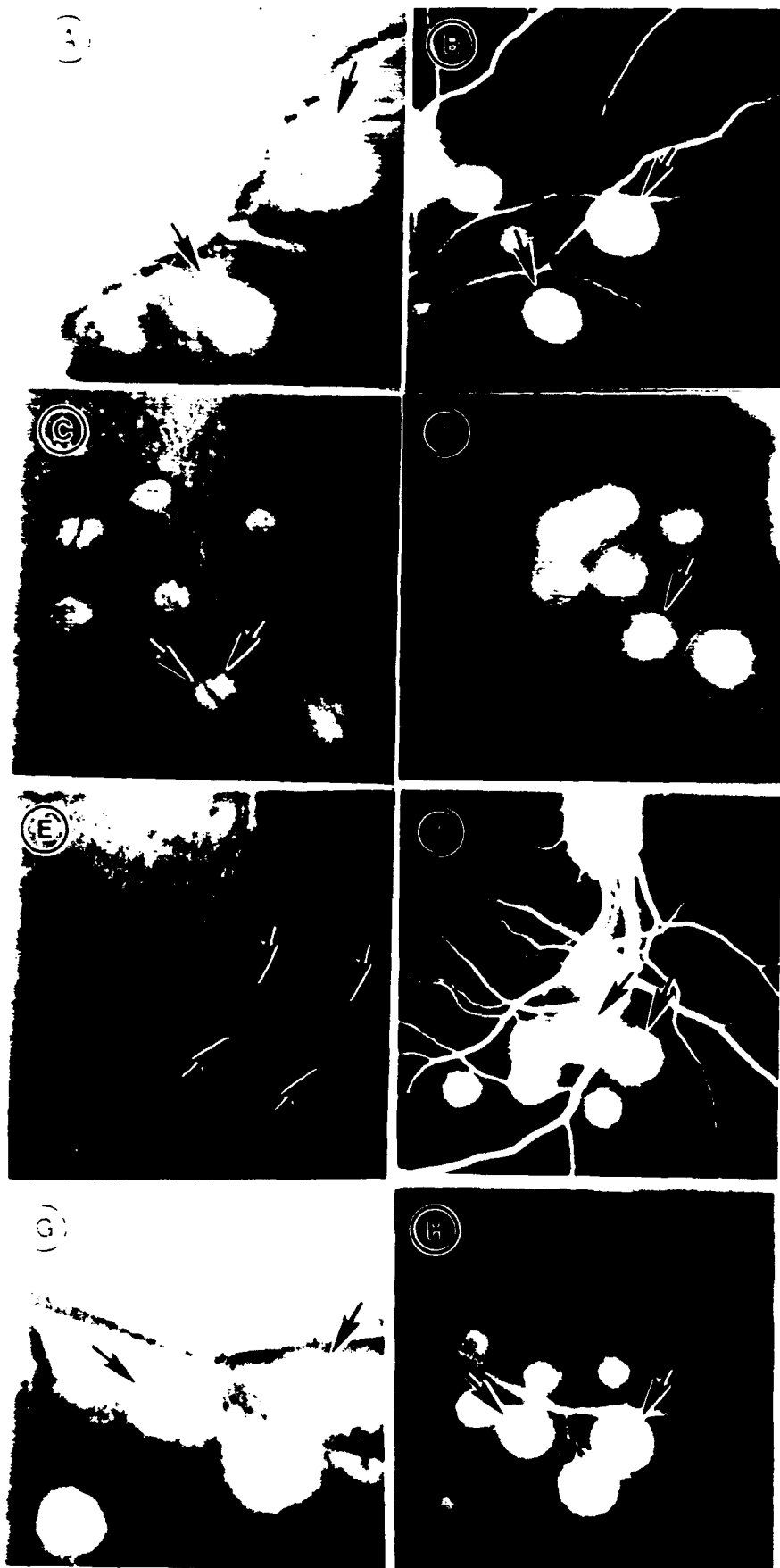


Fig 3.7: Ophthalmoscopic and fluorescein angiographic appearance of Grade III (arrows) lesions in the control (A, B), Treatment Regimen I (C, D), Treatment Regimen II (E, F), and Treatment Regimen III (G, H) groups at 10 days after laser exposure. Retinal lesions of varying severity (Grade II and Grade III) were inflicted by CW Argon laser in the posterior retina of Cynomolgus monkeys and only those of Grade III (arrows) were illustrated. For description, see text 3.4.2.1.

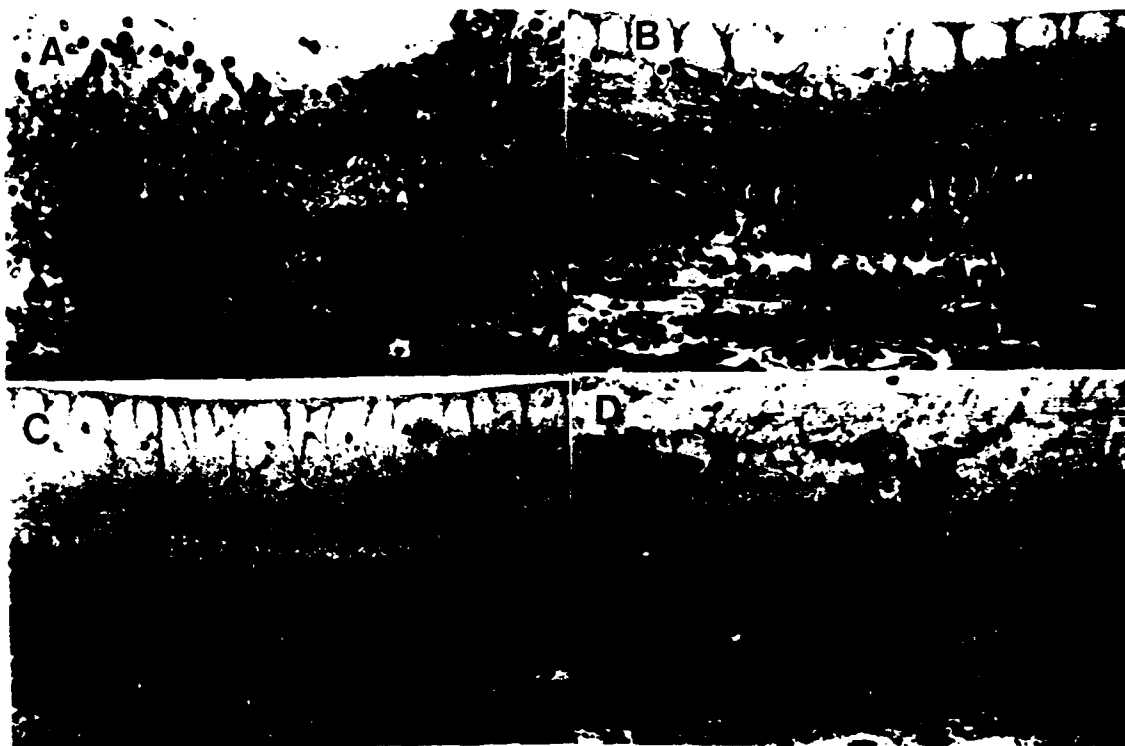


Fig 3.8 **Histopathologic studies of retinal lesions of:**
 (A) Control
 (B) Treatment Regimen I
 (C) Treatment Regimen II
 (D) Treatment Regimen III

For description, see text 3.4.2.2.

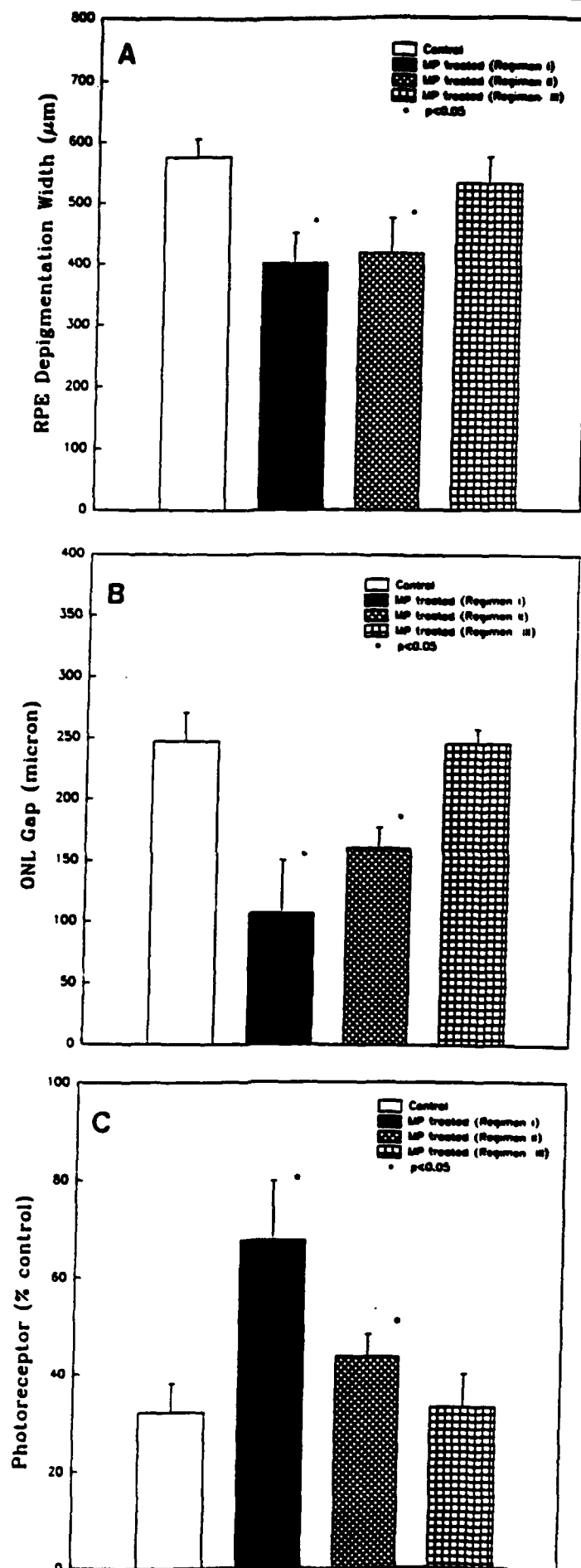


Fig 3.9: The effects of different treatment regimens on laser-induced lesions: (A) the width of depigmented RPE area; (B) outer nuclear layer gap; and (C) the percentage of the remaining photoreceptor nuclei measured at 10 days after the initial insult.

Chapter 4

Ultrastructural modification by high dose methylprednisolone on laser-induced injury of the monkey retina

4.1 Introduction

Pharmacologic studies of disease processes not only provide information on the therapeutic value of the test agents but also insight to the mechanism of drug actions. Since we observed a beneficial effect of MP in non-hemorrhagic retinal laser injury (Chapter 3), we decided to conduct ultrastructural studies with electron microscopy to examine the lesions after injury to gain further insight into the tissue and cellular responses with and without drug treatment. Findings were grouped into observations in the central, peripheral, and paralesional areas of the lesions examined.

4.2 Method

The methods were the same as in Chapter 3. The animals were given treatment regimen I; namely prophactic and continuous methylprednisolone treatment for 4 days and showed the most beneficial effects of treatment by clinical, histopathologic and morphologic criteria. Electron microscopic examination was done on lesions of 3 and 10 days after laser injury. The most representative retinal lesions were selected from each group and thin sections were obtained on the 75/300 nickel grids. They were stained with uranyl acetate and lead citrate, and were examined by electron microscopy (Hitachi 600, Hitachi, Tokyo, Japan). For the purpose of description, the laser lesions were divided into three regions, namely, center of the lesion, periphery of the lesion and paralesional area. Electron micrographs were taken from each areas and compared between control and MP treated groups.

4.3 Results

4.3.1 Ultrastructural features of retinal lesions three days after laser injury

4.3.1.1 Center of the laser-induced retinal lesions

Control lesions

Under the electron microscope, (Fig 4.1A,B), the choriocapillaries (CC) were completely occluded by thrombi composed of red blood cells, polymorphonuclear leukocytes, platelets and fibrin. The endothelial cells of the CC were necrotic with granular cytoplasm and pyknotic nuclei, but the basement membrane of the CC were still continuous. The collagenous and elastic layers of Bruch's membrane appeared intact. The plasmalemma and nuclear membrane of the RPE were

totally disrupted and the watery cytoplasm showed granular appearance but the melanin granules remained along the apices of the cells. The outer and inner segments also showed focal densification in the disc lamellae (Fig 4.1B). The ONL, INL, and the OPL were collapsed and were not identifiable ultrastructurally. Macrophages migrating into these necrotic area were characterized by numerous phagosomes containing the degenerated outer segments and necrotic cellular debris but few melanin granules (Fig 4.1B).

Treated

The CC were completely occluded with necrosis of the endothelium, and fibroblast-like cells were seen in the vascular lumen (Fig 4.2A,B). The RPE showing granular appearance with loss of membranous cytoplasmic structures. Focal densification of the disc membrane structure of the outer and inner segments showed (Fig 4.2B), and the macrophages with phagocytized degenerated inner and outer segment were noted (Fig 4.2A).

4.3.1.2 Periphery of the laser-induced retinal lesions

Control

Under electron microscopy (Fig 4.3A,B), the choriocapillaris at the periphery of the lesion was occluded by thrombi. The proliferating RPE cells with few melanosomes and abundant mitochondria and cellular organelles were seen posterior to the necrotic RPE (Fig 4.3B). The macrophages phagocytized melanin granules and cellular debris and approached to the OLM in the subretinal space (Fig 4.3A). The shrunken photoreceptor cells with densified cytoplasm and pyknotic nuclei were surrounded by intricately interdigitated processes of the Muller cells. The outer limiting membrane consisting of zonula adherent-like cell junction showed focal disruption (Fig 4.3A). In the OPL, loss of axons of the photoreceptor cells and Muller cell processes containing degenerated synaptic terminals with densified cytoplasm and numerous microvacuoles (Fig 4.4A).

Treated

The CC were partially occluded by the thrombi but the lumen of the CC was patent (Fig 4.5A,B). The RPE cells with abundant intracytoplasmic melanin granules were beneath the necrotic RPE. There was very few pigment-laden macrophages in the subretinal space (Fig 4.5B) when compared to the control group (Fig 4.3B). The relatively intact photoreceptor cells at the edge of the lesion showed condensation of the cytoplasm. However, the OLM was well preserved in this area.

4.3.1.3 Paralesional area

Control

In the paralesional area, the axons and synaptic terminals of the photoreceptor cells were

not well aligned, and a noticeable decrease in the number of cone pedicles was in this region (Fig 4.4B).

Treated

In the paralesional area, there were more cone pedicles and rod spherules in the OPL when compared to the control group (Fig 4.6).

4.3.2 Ultrastructural features of retinal lesions ten days after laser injury

4.3.2.1 Center of laser-induced retinal lesions

Control

Ultrastructurally, (Fig 4.7A,B), the choriocapillaris were completely occluded in the region of the lesion. Endothelial cells of the CC were lost and invasion of the fibroblast-like cells were observed in the confine of the remnant basement membrane of the CC. Macrophages invaded between the remnant basement membrane of the RPE and inner collagenous zone of the Bruch's membrane (Fig 4.7B). The proliferated RPE cells showed nuclei with dispersed chromatin and invaginated nuclear membrane. Occasionally, RPE with prominent nucleoli and reticular appearance were also seen. Numerous mitochondria and cytoplasmic organelles but few melanin granules were noted in the cytoplasm of the RPE. Short microvilli of the RPE cells were still present on the apices of the cells, while the basal infolding were lost in most cells. Only a few intercellular junctions were identified between these proliferated RPE cells (Fig 4.7B). The macrophages in the degenerated inner retinal layers were characterized by nuclei with marginated chromatin and abundant phagosomes containing degenerated outer segments, melanin granules and necrotic cellular debris. The cell processes of these macrophages were short and interdigitated with microvilli of the RPE cells or Muller cells (Fig 4.7A,B). There was total loss of the photoreceptor cells and OPL at the center of the lesion, and the neuronal cells of the INL were prolapsed into the outer retinal layers. The cell processes of the Muller cells extended among these prolapsed neuronal cells. The OLM were totally absent at the center of the lesion (Fig 4.7B). The cytoplasm of the Muller cells approximated the microvilli of the RPE cells at the center of the lesion. These Muller cell processes showed complicated interdigitation, abundant mitochondria and glycogen granules. The retinal capillaries in the INL showed loss of the endothelium and pericytes and the vascular lumen was totally occluded. Degenerated dendrites and axons were seen in the IPL (Fig 4.7A).

Treated

The CC were patent showing re-endothelialization with duplicated basement membrane. The lumen of these choriocapillaries were narrow and endothelial cells showed few fenestration (Fig 4.8C). Bruch's membrane and invaginations of the nuclear membrane of the proliferated RPE

cells were remarkable, and prominent nucleoli of RPE cells were rarely seen. The cytoplasm of the RPE cells showed abundant mitochondria, cytoplasmic organelle and dispersed small melanin granules. However the number of the melanin granules was more abundant in this group than in the control group. Microvilli of the RPE cells were longer and more abundant than those of the control groups and were present in the lateral membrane of the cells. Basal infoldings of the RPE cells were well formed, and intercellular junctions between these proliferated RPE cells were abundantly with presence and in the basal and apical portion of the lateral plasmalemma (Fig 4.8C).

The nuclei of the macrophages in the subretinal space were similar to those in the control group, but the total number of the number of phagosomes and phagosomes containing the degenerated outer segments or necrotic debris were much less than those of the control group (Fig 4.8C).

In the reformed OLM, there were numerous zonula adherens-like cell junctions between Muller cell processes. Long cellular processes of the Muller cells extended into the subretinal space. Proteinous subretinal fluid was seen in the subretinal space (Fig 4.8B,C). In the ONL, the remaining photoreceptor cells were surrounded by the cytoplasm of the Muller cells which had abundant microtubules and glycogen granules in the cytoplasm (Fig 4.8B). Surviving photoreceptor cells in the ONL occasionally showed short inner segments and disorganized outer segments, and had densified cytoplasm (Fig 4.8B). The retinal vessels in the INL were patent, however the endothelium shows various grade of degeneration and increase in the pinocytotic vesicles (Fig 4.8A).

4.3.2.2 Periphery of laser-induced retinal lesions

Control

Ultrastructurally, degenerated synaptic terminals of the photoreceptor cells were noted in the OPL which was partially replaced by the processes of the Muller cells (Fig 4.9A).

Treated

Under electron microscopy, a number of the well preserved rod spherules were seen. However the first cone pedicles by the edge of the lesion was condensed showing dilated synaptic vesicles and few synaptic ribbons. Shrunken postsynaptic neuronal cells with pyknotic nuclei and densified cytoplasm were seen in the INL (at close proximity) to such degenerated synaptic expansions (Fig 4.10A). There were also swollen neuronal cells with watery cytoplasm and swollen axons in the INL.

4.3.2.3 Paralesional area

Control

There were areas where only rod spherules were seen at the edge of the lesion. The first identifiable cone pedicle away from the edge of the lesion were densified with microvacuolation. However, the synaptic vesicles and synaptic ribbons were recognizable. Swollen neuronal cells with watery cytoplasm and axons were observed in the INL (Fig 4.6A, 4.6B).

Treated

The synaptic terminals of the cone and rod cells were well aligned and showed good preservation (Fig 4.11B).

4.4 Comments

In this study, we demonstrated the ultrastructural modification following administration of MP in choroidal and retinal blood vessels RPE cells, macrophages, Muller cells, and neuronal cells in the retina by methylprednisolone. These observations further confirmed that the beneficial effects of high doses of MP treatment may be due to its multiple sites of actions on various cellular components of the retina after laser injury. In addition, these findings are consistent with our hypothesis that cellular changes after laser injury can be modulated by pharmacological agents to limit secondary cell death to give a more favorable clinical, pathological, and probably functional outcome.

4.4.1 Effects on choroidal vessels

There was little difference in the pathologic changes in the choriocapillaris at the center of the lesion at 3 days after laser injury between control and MP-treated retinas. However, at 10 days, the control retinal lesion showed complete choroidal vascular occlusion while the blood flow of the retinal and choroidal vasculatures was rapidly re-established in the MP-treated retina, and the vascular lumen was patent. However, the recanalized patent choriocapillaris in the treated group showed duplicated basement membrane, decreased fenestration of the vascular endothelial cells and narrow lumen. Recanalization of the choriocapillaris was previously described by Perry and Risco^{32,33} with transmission electron microscopic and vascular cast techniques in choroidal microvascular recanalization in cat eyes at three months after argon laser photocoagulation using similar exposure settings (500 um, 0.2 sec, 800 um W). Similarly, Katoh et al³⁴ also reported the total recanalization of the choriocapillaris at three months after argon laser photocoagulation in monkey eye in much milder laser lesions. Our observation suggested that MP treatment appears to promote rapid microvascular repair in the choroid and retina. This observation is consistent with the proposal by Hall et al that high doses of glucocorticoids enhances blood flow in injured spinal cord³⁰. The choroidal and retinal vascular effect by MP may be partially responsible for the preservation of the retina after the laser injury. However, direct vasodilator action, changes in adrenergic receptor sensitivity, inhibition of vasoactive prostaglandin formation and inhibition of

endothelial lipid peroxidation might also be involved in the pharmacological actions of MP.³⁰ Specifically, Naven et al³⁵ demonstrated that corticosteroid decreased prostaglandin E2 in laser retinal lesions.

4.4.2 Effects on RPE

The modulation of the repairing process of the RPE cells by MP was remarkable. In the MP-treated retina, a single-layer of the RPE cells with regularly arranged cell junctions relined Bruch's membrane while the control retina showed multi-layers of irregular RPE proliferation with a few randomly-arranged cell junctions. The presence of these well-formed regular cell junctions between the proliferated single-layered RPE cells in the treated group provided an explanation to the clinical observation of the minimal retinal fluorescein leakage at 10 days after laser injury. In addition, the RPE cells in the MP-treated retina had lateral microvilli and basal infolding. The lateral microvilli and basal infolding might probably play a role in the rapid absorption of the subretinal fluid in the retinal lesions. Such differences in the repairing process of the pigmented epithelial barrier were observed between mild laser lesion and severe laser lesions by Wallow³⁶. It appears that MP promoted the rapid reforming of the outer blood retinal barrier. However, Koutsandrea et al³⁷ recently reported the inhibitory effect of RPE proliferation by steroid in the culture. It is possible that moderation of the reactive proliferation of the RPE may better differentiate and lead to a regular mono-layer of RPE cells with tight blood retinal barrier instead of papillary proliferation of RPE without reformation of the blood-retinal barrier.

4.4.3 Effects on macrophagic response

Under light microscopy, there were little differences between the control and MP-treated retina at 3 days after laser injury, but the number of the macrophages in the inner retinal layers were conspicuously less at 10 days after laser injury in the MP-treated animal. In addition, the ultrastructural features of the phagosomes in the macrophages were different between the two groups. In the control retina, the repairing processes were characterized by the clearance of necrotic debris by a large number of macrophages containing a considerable amount of cellular debris. In contrast, the MP-treated retina had less number of the macrophages and less amount of degrading materials in the phagosomes. The effects of glucocorticoids on monocytes and macrophages have been well described in the literatures^{38,39}. These effects on monocytes and macrophages included (1) profound depletion of these cells from blood, (2) alteration of cellular surfaces, (3) diminished response to chemotactic factors, lymphokines, and macrophage activation factor, (4) inhibition of ability to phagocytize, (5) inhibition of pyogene production and (6) inhibition of the secretion of collagenase, elastase and plasminogen activator. The phagocytotic and migrational activities of the macrophages were appeared to be decreased by MP in our study.

These inhibitory effects of MP macrophages might aid in minimizing additional photoreceptor cell loss in the surrounding retinal tissue during the reparative phase after laser injury.

4.4.4 Effects on Muller cells

Specific effects of glucocorticoid to Muller cells is not known. However, we observed a rapid reformation of the OLM by Muller cells. This might be a phenomenon secondary to the suppression of macrophagic infiltration in the MP-treated retina and diminished tissue degradation by the lytic enzymes secreted by the macrophages in the inner retinal layers. Conversely, a rapid reformation of the OLM could establish cytological barrier against the additional infiltration of the macrophages into the inner retinal layers hence lessening the secondary damages to the inner retina.

4.4.5 Effects on photoreceptor cells

The photoreceptor cells in the periphery of the lesion were relatively well-preserved in the MP-treated retina at 3 days after laser injury when compared to the control retina, and these rescued photoreceptor cells appeared to fill in the gap of the outer nuclear layer in the repairing process. This phenomenon was well-documented by morphometric measurements in the previous chapter. In this study, at the periphery of the lesion, degeneration of the synaptic expansion was less in the MP-treated retina and the synaptic expansions in the paralesional area were well preserved in the MP-treated retina. This preservation of the synaptic expansions was consistent with the protective effect of MP on photoreceptor cells. Furthermore, at both 3 and 10 days after laser injury, more cone pedicles were seen in the OPL in the paralesional area in the treated retina while the control retina showed loss of synaptic expansion, especially cone pedicles.

Since secondary degeneration of the synaptic expansions of photoreceptor cells^{16,19} and elongation of the axons of the photoreceptor cells after photocoagulation²⁰ were proposed, the number and morphology of the synaptic expansions in the edge of the lesion and paralesional area are important clues for evaluation of the photoreceptor damage. It is known that cone cells were more susceptible than rod cells in the argon laser photocoagulation¹⁸. Our study suggested that cone cells in the edge of the lesion were also rescued by MP treatment.

4.4.6 Summary

In summary, the rescuing effect of MP on photoreceptors may be due to multiple factors such as its effects on retinal and choroidal vasculatures, RPE blood-retinal barriers, and macrophages and Muller cells. However, it has been demonstrated that intravenously administered high dose MP (15 to 30 mg/kg) can reduce lipid peroxidation in the neuronal cells in cat spinal cord injury³⁰. The direct effect of MP on neuronal lipid peroxidation has been

suggested in a number of studies, and prevention of neurofilament degradation²⁷ and retardation of axonal degeneration²⁸ were reported.



Fig 4.1: Center of the control lesion at 3 days after laser photocoagulation. **A.** The outer and inner nuclear layers were collapsed and macrophages phagocytized cell debris (asterisk) migrated in the necrotic retina. The necrotic inner segments (IS) showed granular appearance. Axons and dendrites of the inner plexiform layer (IPL) showed densification (x4312). **B.** The choriocapillaries were occluded by thrombi consisting of polymorphonuclear leukocytes (PMN) and red blood cells (RBC). The nucleus of the endothelial cell (En) was pyknotic. The RPE cells showed complete necrosis and outer segment (OS) showed focal densification in the lamellae. BM: Bruch's membrane (x4110).

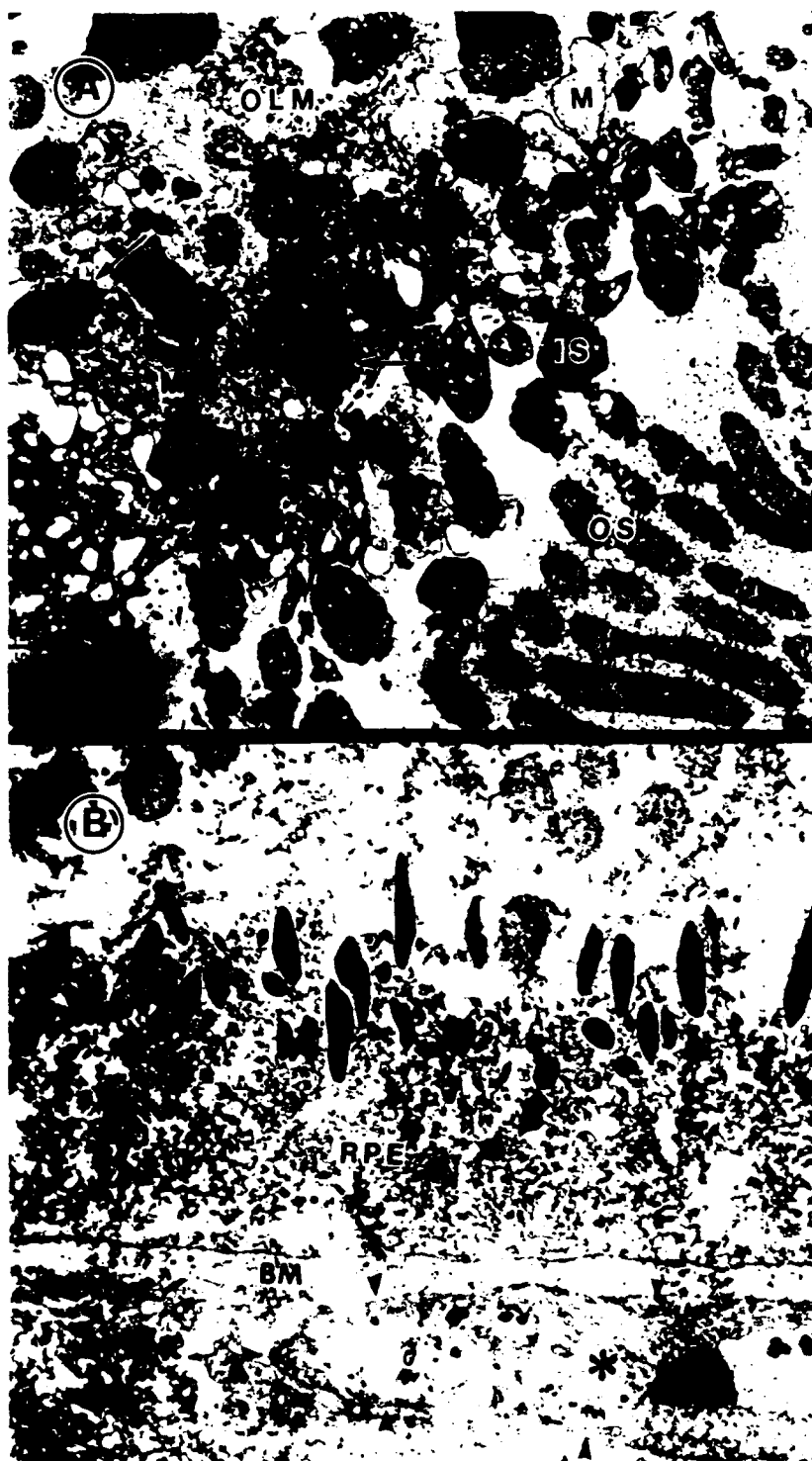


Fig 4.2: Center of the MP-treated lesion at 3 days after laser photocoagulation. **A.** The outer nuclear layer. The macrophages (M) migrated beneath the outer limiting membrane (OLM) phagocytizing the necrotic inner and outer segments (IS and OS). Arrows shows phagocytized inner and outer segments (x3245). **B.** The choriocapillaris and RPE cells. The choriocapillaris showed occlusion with necrosis of the endothelial cells and fibroblast-like cell (asterisk) in the lumen. Basement membrane of the choriocapillaris (arrowheads) was continuous. RPE cells were totally necrotic. BM: Bruch's membrane. (x5650)

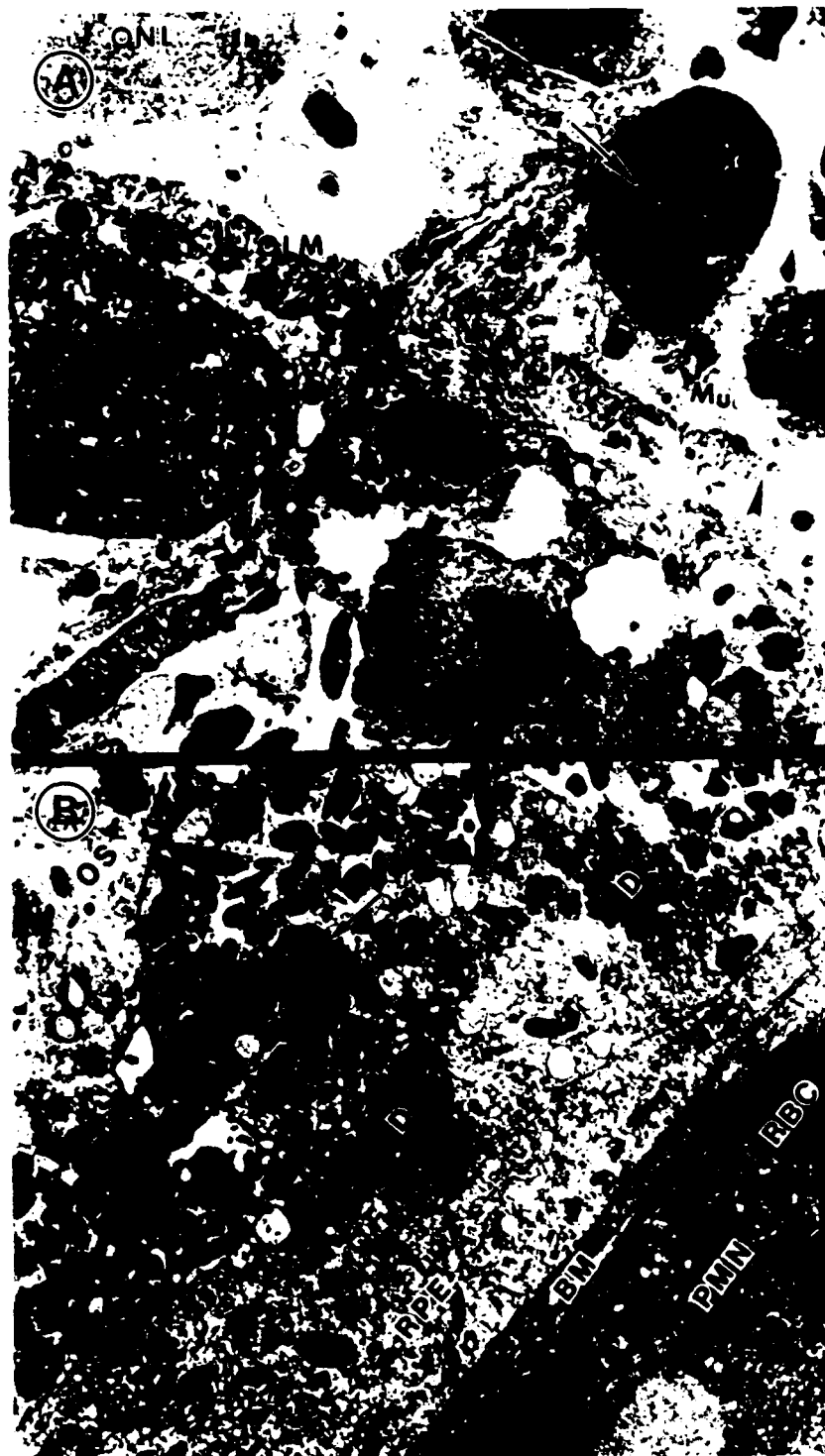


Fig 4.3: Periphery of the control lesion at 3 days after laser photocoagulation. A. the outer nuclear layer (ONL) showed shrunken photoreceptor cells with densification (arrow) which was surrounded by processes of the Muller cells (Mu). The outer limiting membrane (OLM) was disrupted at the central side of the lesion (arrowhead). The macrophage (M) approached to the outer limiting membrane. IS: degenerated inner segment. (x4702). B. The choriocapillaris was occluded by thrombi and RPE cells with abundant organelles were seen beneath the debris (D) of the necrotic RPE cells. Macrophages (M) with degenerated outer segments (arrow) and cellular debris were noted above the RPE cells. OS: outer segment. BM: Bruch's membrane (x5134)



Fig 4.4: The outer plexiform layer in the control lesion at 3 days after laser photocoagulation. A. Periphery of the lesion. Axonal loss of photoreceptors was apparent. Processes of the Muller cells (Mu) enveloped the degenerated synaptic terminals (arrows). The outer nuclear layer (ONL) showed pyknotic nuclei. (x4759) B. Paralesional area. The axons and synaptic terminals (r = rod spherule, c = cone pedicle) of the photoreceptor cells were not well-aligned. The cone pedicles were especially few in number (x2836).



Fig 4.5: Periphery of the MP-treated lesion at 3 days after laser photocoagulation. Outer nuclear layer (ONL). A relatively intact cone cells with condensation of the cytoplasm were seen. Inner segment of the cone cell was also condensed. The outer segment (OS) showed disruption and densification. Outer limiting membrane (OLM) was continuous (x2250). B. The choriocapillaris and RPE cells. The lumen of the choriocapillaris was patent (CC). The RPE cells with abundant melanin granules migrated beneath the Debris of the necrotic RPE cells (D). No macrophages were seen in this area. arrows: densified outer segment (x3811).



Fig 4.6: The outer plexiform layer of the paralesional area in the control lesion at 3 days after photocoagulation. Cone pedicles (c) were well preserved and well aligned with rod spherules (r). INL: inner nuclear layer, ONL = outer nuclear layer (x3304).



Fig 4.7: Center of the control lesion at 10 days after laser photocoagulation. A. The inner nuclear layer and inner plexiform layer (IPL). Macrophages with abundant phagosomes migrated into the inner nuclear layer. The retinal capillaries (arrows) showed various grade of occlusion. Axons and dendrites in the IPL were vacuolated (x3345). B. The choriocapillaris and RPE. The choriocapillaris was occluded and fibroblast-like cell was seen in the vascular lumen. Bruch's membrane (BM) showed separation of the basement membrane of the RPE cells (bm), and macrophage (M) migrated between them. The RPE cells showed multilayered proliferation with few intercellular junctions (arrows). Many macrophages with abundant phagosomes were seen in the subretinal space. N: herniated neuronal cells in the inner nuclear layer, Mu: Muller cell processes (x2976).



Fig 4 8: The center of the MP-treated lesion at 10 days after laser photocoagulation. A) The retinal capillary in the inner nuclear layer (INL). The endothelial cells showed myelin figure & increased pinocytotic vesicles, yet the lumen was patent. The outer plexiform layer (OPL) showed loss & degeneration (arrowhead) of synaptic expansion in this area (x4974). B) The outer nuclear layer (ONL) showed surviving photoreceptor cells with short inner segment (IS) & disorganized outer segment (OS). The outer limiting membrane (OLM) was composed of continuous zonula adherens like junctions. Long processes of the Muller cells opposed to the subretinal space (x4875). C. The choriocapillaris (CC) & RPE cells. The (CC) was patent & the RPE cells showed monolayer regular proliferation forming multiple intercellular junctions (arrows). The subretinal space was free from macrophages. BM: Bruch's membrane. OLM: outer limiting membrane (x3782). Upper inset: The macrophages in the subretinal space showed fewer phagosomes (x3706). Lower inset: the CC with duplicated basement membrane (arrowhead) few fenestration (x2700).



Fig 4.9: The outer plexiform layer (OPL) in the control lesion at 10 days after photocoagulation. A. Periphery of the lesion. The inner part of the OPL was replaced by processes of the Muller cells (Mu). Degenerated synaptic terminals (arrows) were still seen. The inner nuclear layer (INL) showed neuronal cells with watery cytoplasm (asterisk) (x4818). B. Paralesional area. The cone pedicles (c) were densified with microvacuolation (arrowheads). Postsynaptic neuronal element also showed degeneration with microvacuolation. r: rod spherules. (x4851)



Fig 4.10: The outer plexiform layer in the MP-treated lesion at 10 days after laser photocoagulation. **A.** Periphery of the lesion. The rod spherules (r) appeared relatively intact, however the first cone pedicle (c) showed densification. Degenerated postsynaptic neuronal element (asterisk) was seen adjacent to the degenerated cone pedicle. The inner nuclear layer (INL) showed condensed degenerated cells with pyknotic nuclei in the outermost layer (arrows). ONL: outer nuclear layer (x3446). **B.** Paralesional area. Synaptic terminals of the cone cells (c) & rod cells (r) were well aligned & showed good preservation (x3611).

Chapter 5

Evaluation of efficacy of t-PA in subretinal hemorrhage induced by retinal laser injury in rats

5.1 Pathophysiology of vitreal or retinal hemorrhage

In severe laser injury, bleeding from retinal or choroidal vasculature may occur, resulting in retinal and/or vitreal hemorrhage.

Of the 23 cases of accidental laser injuries summarized by Wolfe, 11 patients (74%) had hemorrhage. Both cases reviewed in Chapter 2 had retinal/vitreal hemorrhage. It is therefore important to explore new therapeutic modalities for the treatment of hemorrhage in laser injury.

The pathophysiologic process of vitreous hemorrhage has been described in detail in the literature⁴⁰⁻⁴⁷ and will only be briefly summarized. As blood bleeds into the vitreous cavity from the retinal or choroidal circulations, a fibrinous clot is rapidly formed within the vitreous gel probably initiated by platelet aggregation. The extravasated red blood cells are enmeshed in a network of fibrin. Subsequently, fibrinolysis, hemolysis, and phagocytosis follow. Complications such as posterior detachment, liquefaction of the vitreous, formation of vitreous membrane, vitreous neovascularization and vitreous traction bands may occur. In advanced cases, retinal detachment may take place. Hemolytic glaucoma, siderotic glaucoma, and siderosis bulbae may be caused by further degradation of blood components.

Massive subretinal hemorrhage involving the macula is a devastating complication of choroidal trauma. Although visual recovery may be excellent in some patients, the visual prognosis is generally poor. The pathophysiology of subretinal hemorrhage is not well understood. Glatt and Machemer⁴⁷ postulated that a blood clot in the subretinal space damages the overlying retina by forming a metabolic exchange barrier between the retina and the pigmented epithelium and by iron toxicity.

5.2 Treatment of intravitreal and subretinal hemorrhage

Besides surgical removal of intravitreal and subretinal blood⁴⁴⁻⁴⁸, pharmacologic treatment has also been proposed⁴⁹⁻⁶⁷. Retinal damage and other complications associated with intraocular hemorrhage may be reduced by pharmacologic dissolution of the fibrin meshwork within the clot. Clot lysis might also allow more rapid clearance of blood by phagocytic mechanisms. In addition, pharmacologic therapy of sub-retinal hemorrhage might be accomplished with less trauma and fewer complications than those accompanying surgical evacuation.

5.3 Earlier experimental treatments

Fibrinolytic agents such as fibrinolysin streptokinase, urokinase, and t-PA have been

tested⁴⁸⁻⁶⁷. Fibrinolysin and streptokinase were used in experimental hyphema, but complication of corneal edema was seen in treated eyes⁵⁹⁻⁶⁴. Similar results were found in the use of urokinase. Leet examined the effect of urokinase in rabbits in experimental hyphema and showed it to be effective in the clearance of blood and fibrin⁶⁰. Liebman, however, noted that corneal edema occurred in the treated eyes⁶¹. Rakusin reported the clinical use of urokinase in 20 patients with persistent hyphema and showed an accelerated blood clearance⁶². Chapman-Smith and Crocke noted sterile hypopyon and corneal edema after urokinase injection⁶³. Bramsen noted corneal edema and increase in corneal thickness with intravitreal injection⁶⁴. At higher doses, urokinase was noted to cause loss of photoreceptor outer segments and retinal disorganization. Belkin et al have applied urokinase in experimental laser-induced vitreous hemorrhage and noted that urokinase did not accelerate the absorption of blood but did prevent the development of severe vitreous fibrosis¹¹. These investigators suggested that urokinase should be given early before vitreous fibrosis takes place.

5.4 Tissue plasminogen activator (t-PA)

Tissue plasminogen activator (t-PA, a 70-kD serine protease) is a naturally occurring clot specific fibrinolytic agent produced mainly by the human endothelium. It promotes thrombolysis by hydrolyzing the Arg⁵⁶⁰-Val⁵⁶¹ peptide bond in plasminogen to form the active proteolytic enzyme plasmin. This serine protease in turn nonspecifically degrades fibrin, fibrinogen, and other pro-coagulant factors including V, VIII and XII causing fibrinolysis of the fibrin clot. In the literature, t-PA has been reported to accelerate the clearance of blood clot from the vitreous and subretinal space. Lambrou et al has studied the use of t-PA in experimental hyphema and experimental fibrin clot^{65,66}. When t-PA given intracamerally at 24 hours after injection of whole blood into the anterior chamber, it caused little corneal edema and no significant increase in intraocular pressure but showed significant increase in intraocular pressure but showed significant effectiveness (80% clearance within 24 hours in the treated group versus 14 days in the control group) in accelerating the clearance of hyphema in rabbit eyes. Using a gas compression induced intravitreal fibrin clot model, the same investigators reported no significant toxicity as measured by slit lamp biomicroscopy (corneal =I thickness), electroretinography, tonometry (intraocular pressure), and histopathologic examination after intravitreal injection of 25 ug of t-PA. The t-PA treated eyes cleared within 6 hours versus 6 days in the controls. However, in their experiments, only intravitreal fibrin clot was induced in the treated eyes, and vitreous hemorrhage, lysis and removal of red blood cells were not studied. Also, there was no decrease in the complication associated with retinal and vitreal hemorrhage with t-PA treatment. In addition, treatment with t-PA enhanced the chance of further bleeding^{49,53}. However, these studies were performed with models not using laser. Because of the anticipated large variations, there is a need for large sample size.

Since the vasculature of the rat is closer to human than rabbit, we developed a rat model of subretinal hemorrhage to evaluate the efficacy of intravitreal injection of t-PA.

5.5 Method

5.5.1 Preliminary test of experimental parameters

Four eyes of 2 male Long Evans rats (45-50 days, Harlan, Indianapolis, IN) were employed to determine the necessary conditions to generate subretinal hemorrhage. Each animal was given an intraperitoneal injection of 20 mg/kg Nembutal for anesthesia. A custom made rat holder was utilized for restraining and position of the animals. Multiple lesions were inflicted on the rat retina with the same continuous-wave Argon (CW Argon) laser as described in Chapter 3 (Coherent Medical, Palo Alto, CA) attached to a slit-lamp delivery system (Carl Zeiss, Thornwood, NY) and with a custom made contact lens.

Retinal lesions were examined at 7 days after injury and conditions corresponding to subretinal hemorrhage with no vitreous involvement were selected. Results showed that with 0.1 sec duration at an energy setting of 0.60 W, a spot size of 800 micron at the cornea level, reproducible subretinal hemorrhage could be obtained with proper focus.

5.5.2 Efficacy of t-PA in subretinal hemorrhage in rats

Eight eyes of four male Long Evans rats (45-50 days) (Harlan, Indianapolis, IN) were employed for this study. The animals were divided into two equal groups: control and t-PA treated. Both groups were exposed to laser with the settings determined in the previous section. Twenty-four hours after the injury, the animals were given an intravitreal injection of 25 μ l of sterilized water or 25 μ g of t-PA in the same volume for the control and treated groups respectively. Animals were killed by Nembutal overdose four days after laser injury and their eyes were enucleated. The retinas were fixed in 4% paraformaldehyde and 1% glutaraldehyde, postfixes in alcohol, and embedded in epoxy resin. One-micron serial sections were cut until the center of the lesions was reached, as defined in Chapter 3.

5.5.3 Evaluation

The extent of the sub-retinal hemorrhage was difficult to quantitate as blood tended to spread anteriorly or laterally. For an approximate index, we took the distance from the center of the lesion to the edge of the hemorrhage spot. Further refinement of this index will be needed.

5.6 Results

Figure 5.1 showed typical histologic sections of control (A) and t-PA (B) treated retinal

lesions with subretinal hemorrhage induced by Argon laser in rat. At the center of the lesions, the choriocapillaries were occluded. The RPE, photoreceptor layer, outer nuclear layer, outer plexiform layer, and inner nuclear layer were necrotic. Aggregates of macrophages were noted at the damaged area. The severity of the injuries was comparable between control and treated.

Figure 5.2 depicts the morphometric measurements with and without 25 ug t-PA treatment. The t-PA treatment gave a smaller value in the extent of sub-retinal hemorrhage. However, there was no statistical significance between the two.

5.7 Comments

This study represents a first attempt to quantitatively evaluate the efficacy of recombinant t-PA on subretinal hemorrhage induced by laser in a rat model. Our results, though small in sample size, suggested that single intravitreal injection of 25 ug of recombinant t-PA did not accelerate the clearance of blood from the subretinal space. However, factors such as different morphometric indices, dosage, time of injection, and time point of observation should also be investigated to rule out possible beneficial effects of t-PA in subretinal hemorrhage by laser injury.

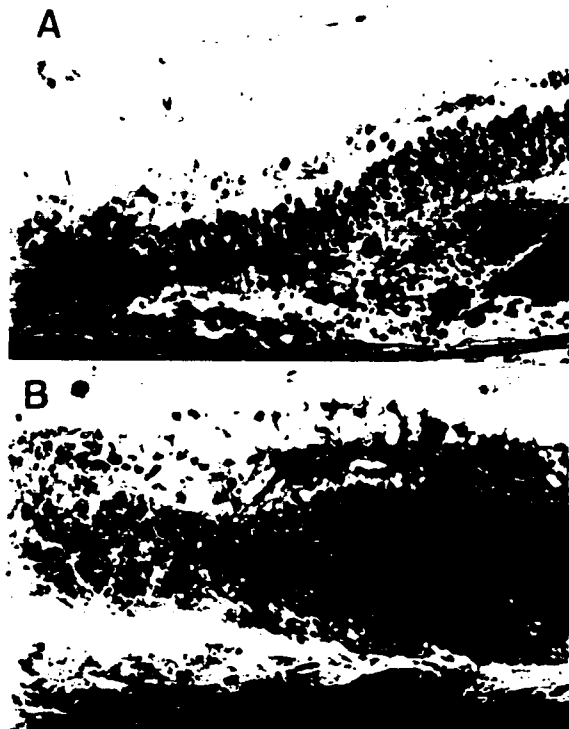


Fig 5.1: Histologic section of Control (A) and t-PA-treated (B) subretinal hemorrhage lesions.

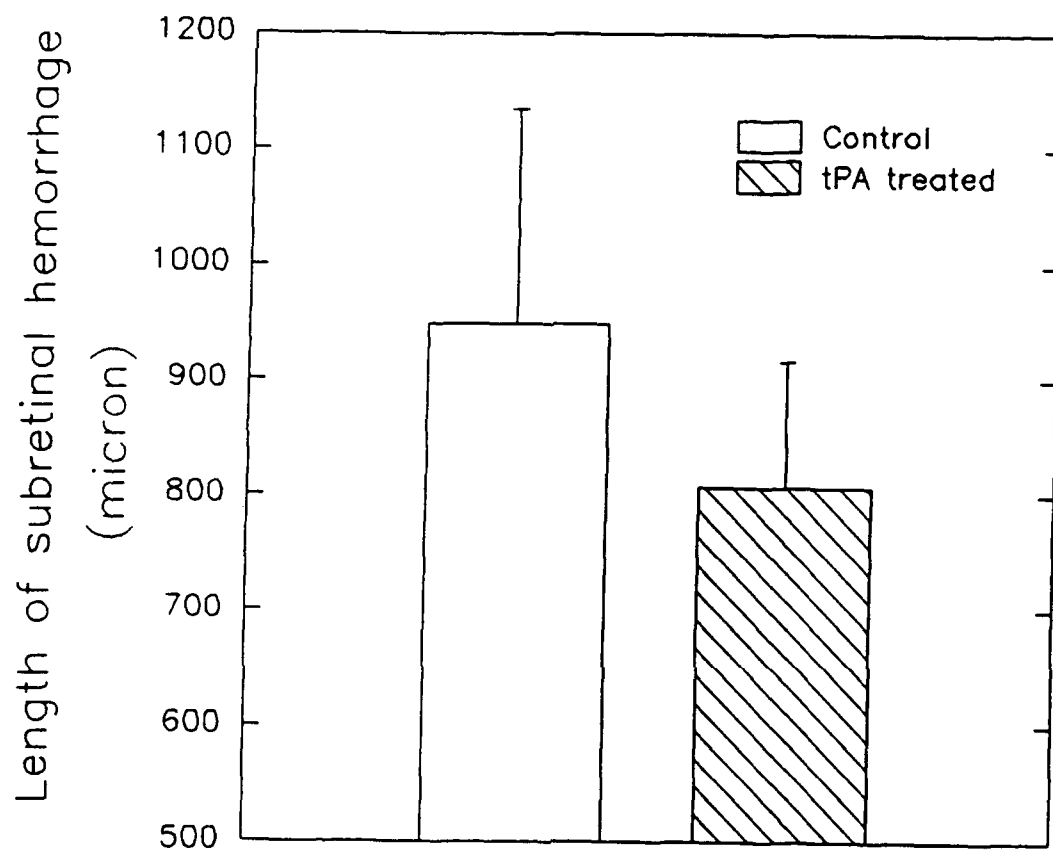


Fig 5.2 Morphometry of laser lesions with subretinal hemorrhage with and without t-PA treatment (25 ug).

CONCLUDING REMARKS

1. We established a subhuman primate model for quantitative evaluation of the effects of pharmacologic agents on retinal laser injury.
2. We examined 3 different regimens of high doses (30 mg/kg loading and 5.4 mg/kg/hr maintenance) of methylprednisolone on Grade III retinal laser injuries with clinical, histopathological, and morphometric criteria. With clinical and histopathological criteria, all three regimens were effective. However, when morphometric indices were included, only regimens I & II (which required a treatment period of 4 days) showed statistical significant beneficial effect.
3. We developed a rat model of subretinal hemorrhage by laser and evaluated the effect of 25 ug t-PA given at 1 day after hemorrhage. There was no beneficial effect under these conditions.
4. Parts of our observations in Chapters 2, 3, and 4 are in the final stage for preparation for publication in peer review ophthalmic journals.

REFERENCES

1. Rathkey AS. Accidental laser burn of the macula. *Arch. Ophthalmol.* 1965;74:346-348
2. Wolfe CJA. Laser retinal injury. *Military Medicine* 1985;150:177-185
3. Kearney JJ, Cohen HB, Stuck BE, Rudd GP, Beresky DE, Wertz FD. Laser injury to multiple retinal foci. *Lasers Surg. Med.* 1987;7:499-502
4. Friedmann AI. A natural clinical history of a severe accidental retinal laser burn at the posterior pole of the eye. *Documenta Ophthalmologica* 1988;68:395-400
5. Anderberg B, Sjolund B, Bolander G, Steinvall O, Tengroth B. Vulnerability of the retina to injury from a military ruby rangefinder at battlefield distances. *Health Physics* 1989;56(5):743-748
6. Gabel V-P, Bringruber R, Lorenz B. Clinical observations of six cases of laser injury to the eye. *Health Physics* 1989;56:705-710
7. Cai Y, Xu D, Mo X. Clinical, pathological and photochemical studies of laser injury of the retina. *Health Physics* 1989;56(5):643-646
8. Liu H, Gao G, Wu D, Xu G, Shi L, Xu J, Wang H. Ocular injuries from accidental laser exposure. *Health Physics* 1989;56/5:711-716
9. Whitacre MM, Mainster MA. Hazards of laser beam reflections in eyes containing gas. *Am. J. Ophthalmol.* 1990;110:33-38.
10. Ishibashi T, Miki K, Sorgente N, Patterson R, Ryan SJ. Effects of intravitreal administration of steroids on experimental subretinal neovascularization in the subhuman primate. *Arch. Ophthalmol.* 1985;103:708-711
11. Belkin M, Lund DJ, Beatrice ES. Urokinase-treatment of fresh laser irradiation-induced vitreous hemorrhage. *Ophthalmologica* 1983;187:152
12. Siesjo BK, Bengtson F, Grampp W, Pheander S. Calcium, excitotoxins, and neuronal death in the brain. *ANYAS* 1989;568:234-251
13. Hall ED, Braughler JM. Central nervous system trauma and stroke II. Physiological and pharmacological evidence for involvement of oxygen radicals and lipid peroxidation. *Free Rad. Bio. Med.* 1989;6:303-313
14. Manning JR, Davidorf DH, Keatus RH, Strange AE. Neodymium-YAG laser lesions in the human retina: accidental/experimental. *Contemp. Ophthalmic Forum* 1986;4:86-91
15. Tso MOM, Wallow IHL, Elgin S. Experimental photocoagulation of the human retina. I. Correlation of physical, clinical, and pathologic data. *Arch. Ophthalmol.* 1977;95:1035-1040
16. Wallow IHL, Tso MOM, Elgin S. Experimental photocoagulation of the human retina. II. Electron microscopic study. *Arch. Ophthalmol.* 1977;95:1041-1050

17. Powell CJO, Tso MOM, Wallow IHL, Frisch GD. Recovery of the retina from argon laser radiation: clinical and light microscopic evaluation. *Ann. Ophthalmol.* 1974;6:1003-1012
18. Tso MOM, Wallow IHL, Powell JO. Differential susceptibility of rod and cone cells to argon laser. *Arch. Ophthalmol.* 1973;89:228-234
19. Marshall J. Thermal and mechanical mechanisms in laser damage to the retina. *Invest. Ophthalmol.* 1970;9:97-114
20. Marshall J. Interactions between sensory cells, glial cells and the retinal pigment epithelium and their response to photocoagulation. *Dev. Ophthalmol.* 1981;2:308-317
21. Marshall J. Structural aspects of laser-induced damage and their functional implications. *Health Physics* 1989;56:617-624
22. Marshall J, Bird A. A comparative histopathological study of argon and krypton laser irradiation of the human retina. *Br. J. Ophthalmol.* 1979;63:657-668
23. Tso MOM: Repair and late degeneration of the primate fovea after injury by argon laser. *Invest. Ophthalmol. Vis. Sci.* 1979;18:447-461
24. Bracken MB, Shepard MJ, Collins WF, Holford TR, Young W et al. A randomized, controlled trial of methylprednisolone or naloxone in the treatment of acute spinal-cord injury. *N. Eng. J. Med.* 1990;322:1405-1411
25. Hall ED, Braughler JM. Glucocorticoid mechanisms in acute spinal cord injury: a review and therapeutic rationale. *Surg. Neurol.* 1982;18:320-327
26. Braughler JM, Hall ED. Current application of "high dose" steroid therapy for CNS injury: a pharmacological perspective. *J. Neurosurg.* 1985;62:806-810
27. Green BA, Kahn T, Klose KJ. A comparative study of steroid therapy in acute experimental spinal cord injury. *Surg. Neurol.* 1980;13:91-97
28. Means ED, Anderson DK, Waters TR, Kalaf L. Effect of methylprednisolone in compression trauma to the feline spinal cord. *J. Neurosurg.* 1981;55:200-208
29. Anderson DK, Saunders RD, Demediuk P et al. Lipid hydrolysis and peroxidation in injured spinal cord: partial protection with methylprednisolone or vitamin E and selenium. *Cent. Nerv. System Trauma* 1985;2:257-267
30. Hall ED, Braughler JM. Effects of intravenous methylprednisolone on spinal cord lipid peroxidation and ($\text{Na}^+ + \text{K}^+$)-ATPase activity: dose-response analysis during the first hour after contusion injury in the cat. *J. Neurosurg.* 1982;
31. Hall ED, Braughler JM. Acute effects of intravenous glucocorticoid pretreatment on the in vitro peroxidation of cat spinal cord tissue. *Exp. Neurol.* 1981;73:321-324
32. Perry DD, Risco JM. Choroidal microvascular repair after argon laser photocoagulation. *Am. J. Ophthalmol.* 1982;93:787-793
33. Perry DD, Reddick RL, Risco JM. Choroidal microvascular repair after argon laser

- photocoagulation. Ultrastructural observation. *Invest. Ophthalmol. Vis. Sci.* 1984;25:1019-1026
34. Katoh N, Ohkuma H, Itagaki T, Yanagishi K, Uyama M. A comparative study of effects of photocoagulation with the argon blue-green and krypton red lasers on the retina and choroid. 3. A scanning electron microscopic study of the choroidal vascular casts. *Acta. Soc. Ophthalmol. Jpn.* 1986;90:898-907
 35. Naven N, Weissman C. Corticosteroid treatment of laser retinal damage affects prostaglandin E2 response. *Invest. Ophthalmol. Vis. Sci.* 1990;31:9-13
 36. Wallow IH. Repair of the pigment epithelial barrier following photocoagulation. *Arch. Ophthalmol.* 1984;102:126-135
 37. Koutsandrea CN, Miceli MV, Peyman GA, Farahat HG, Niesman MR. Ciprofloxacin and dexamethasone inhibit the proliferation of human retinal pigment epithelial cells in culture. *Curr. Eye Res.* 1991;10:249-258
 38. Ishikawa Y. An electron microscopic study on the origin of macrophages in the photocoagulated retina. *Acta. Soc. Ophthalmol. Jpn.* 1978;82:509-516
 39. Gloor BP. On the question of the origin of macrophages in the retina and vitreous following photocoagulation (autoradiographic investigations by means of ^3H -Thymidine) Albrecht V. Graefes *Arch. Klin. Exp. Ophthalmol.* 1974;190:183-194
 40. Gillies A, Lahav M. Absorption of retinal and subretinal hemorrhage. *Ann. Ophthalmol.* 1983;15:1068-1074.
 41. Dellaporta A. Retinal damage from subretinal hemorrhage. *Am. J. Ophthalmol.* 1983;95:568-570
 42. Bennett SR, Folk JC, Blodi CF, Klugman M. Factors prognostic of visual outcome in patients with subretinal hemorrhage. *Am. J. Ophthalmol.* 1990;109:33-37
 43. Wade EC, Flynn Jr HW, Olsen KR et al. Subretinal hemorrhage management by pars plana vitrectomy and internal drainage. *Arch. Ophthalmol.* 1990;108:973-978
 44. Vander JF, Federman JL, Greven C et al. Surgical removal of massive subretinal hemorrhage associated with age-related macular degeneration. *Ophthalmology* 1991;98:23-27
 45. Han DP, Mieler WF, Schwartz DM, Abrams GW. Management of traumatic hemorrhagic retinal detachment with pars plana vitrectomy. *Arch. Ophthalmol.* 1990;108:1281-1286
 46. Hanscom TA, Diddie KR. Early surgical drainage of macular subretinal hemorrhage. *Arch. Ophthalmol.* 1987;105:1722-1723
 47. Glatt H, Machemer R. Experimental subretinal hemorrhage in rabbits. *Am. J. Ophthalmol.* 1982;94:762-773
 48. deJuan Jr E, Machemer R. Vitreous surgery for hemorrhagic and fibrous complications of

- age-related macular degeneration. *Am. J. Ophthalmol.* 1988;105:25-29
49. Johnson MW, Olsen KR, Hernandez E. Tissue plasminogen activator treatment of experimental subretinal hemorrhage. *Retina* 1991;11:250-258
 50. Jaffe GJ, Lewis H, Han DP, Williams GA, Abrams GW. Treatment of postvitrectomy fibrin pupillary block with tissue plasminogen activator. *Am. J. Ophthalmol.* 1989;108:170-175
 51. Vine AK, Maguire PT, Martonyi C, Kincaid MC. Recombinant tissue plasminogen activator to lyse experimentally induced retinal arterial thrombi. *Am. J. Ophthalmol.* 1988;105:266-270
 52. Williams DF, Bennett SR, Abrams GW, Han DP, Mieler WF, Jaffe GJ, Williams GA. Low-dose intraocular tissue plasminogen activator for treatment of postvitrectomy fibrin formation. *Am. J. Ophthalmol.* 1990;109/5:606-607
 53. Johnson RN, Olsen KR, Hernandez E. Intravitreal tissue plasminogen activator treatment of experimental vitreous hemorrhage. *Arch. Ophthalmol.* 1989;107:891-894
 54. Sternberg P, Aguilar HE, Drews C, Aaberg TM. The effect of tissue plasminogen activator on retinal bleeding. *Arch. ophthalmol.* 1990;108:720-722
 55. Toth CA, Morse LS, Hjelmeland LM, Landers MB III. Fibrin detects early retinal damage after experimental subretinal hemorrhage. *Arch. Ophthalmol.* 1991;109:723-729
 56. Oncel M, Peyman GA, Khoobehi B. Tissue plasminogen activator in the treatment of experimental retinal vein occlusion. *Retina* 1989;9:1-7
 57. Liu JC, Peyman GA, Oncel M. Treatment of experimental suprachoroidal hemorrhage with subconjunctival injection of tissue plasminogen activator: A negative report. *Ophthalm. Surg.* 1990;21/9:641-643
 58. Forrester JV, Edgar W, Prentice CRM, Forbes CD, Williamson J. Intravitreal fibrinolysis in experimental vitreous hemorrhage. *Expt. Eye Res.* 1976;27:181-188
 59. Maberly AL, Chisholm LDJ. The effect of fibrinolytic agents on vitreous hemorrhage in rabbits. *Can. J. Ophthalmol.* 1970;5:55-64
 60. Leet DM. Treatment of total hyphemas with urokinase. *Am. J. Ophthalmol.* 1977;84:79-84
 61. Liebman SD, Pollen A, Podos SM. Treatment of experimental total hyphema with intraocular fibrinolytic agents. *Arch. Ophthalmol.* 1962;68:102-108
 62. Rakusin W. Urokinase in the management of traumatic hyphema. *Br. J. Ophthalmol.* 1971;55:826-832
 63. Chapman-Smith JS, Crock GW. Urokinase in the management of vitreous hemorrhage. *Br. J. Ophthalmol.* 1977;61:500-505
 64. Bramsen T. Fibrinolysis and traumatic hyphema. *Acta. Ophthalmol.* 1979;57:447-454
 65. Lambrou FH, Snyder RW, Williams GA, Lewandowski M. Treatment of experimental intravitreal fibrin with tissue plasminogen activator. *Am. J. Ophthalmol.* 1987;104:619-623

66. Lambrou FH, Snyder RW, Williams GA. The use of tissue plasminogen activator in experimental hyphema. *Arch. Ophthalmol.* 1987;105:995
67. Lewis H, Resnick SC, Flannery JG, Straatsma BR. Tissue plasminogen activator treatment of experimental subretinal hemorrhage. *Am. J. Ophthalmol.* 1991;111:197-204

ACKNOWLEDGMENTS

We gratefully acknowledge the encouragement of program manager L. N. Durvasula of the DARPA Defense Science Office. We thank B.E. Stuck of the Letterman Army Institute of Research and M. Belkin of Israel for helpful discussion and advice.

T. T. Lam, K. Takahashi and J. Fu led the effort in this study. This report was written by T. T. Lam and M. O. M. Tso. Dr. Tso is the principal investigator of this project.

We acknowledge the technical support by I. Suvaizdis, K. Kim, M. Mori and secretarial/administrative assistance of B. Gordon and K. Stojack.